

Jets and flow in relativistic heavy-ion collisions

Guang-You Qin (秦广友)

Central China Normal University

华中师范大学

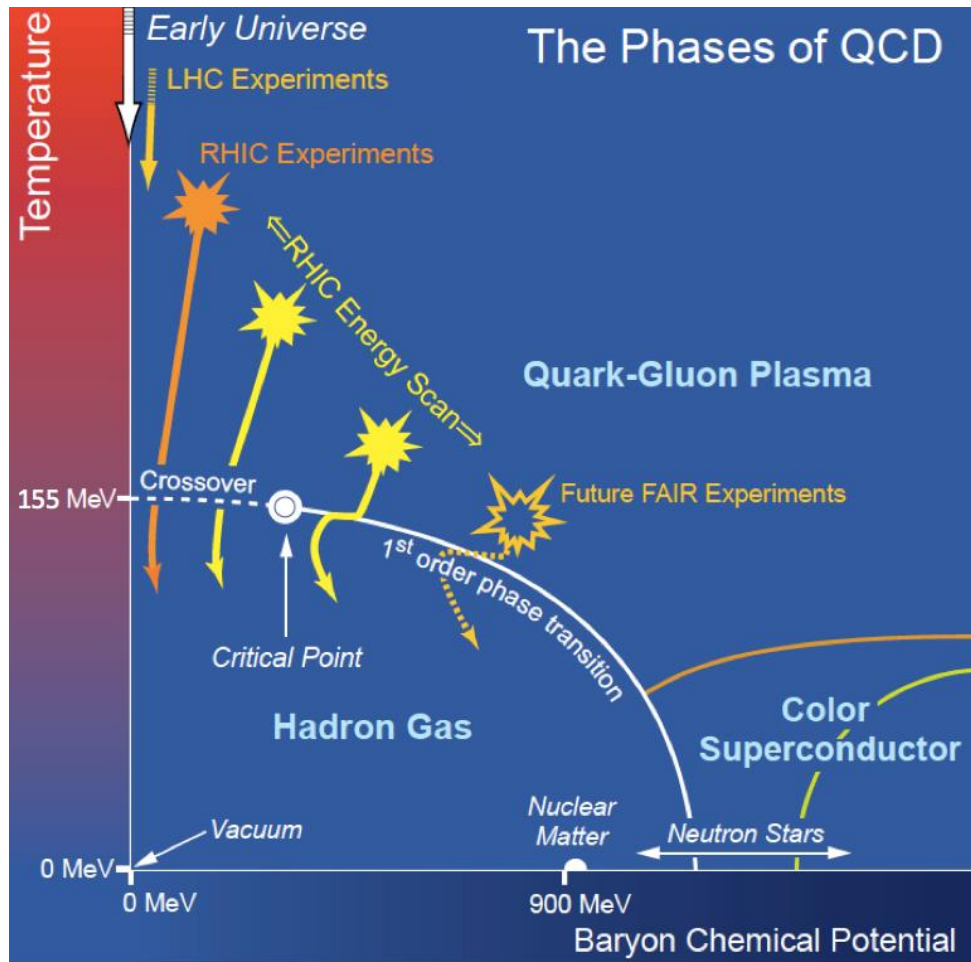
中国科学技术大学

2021年4月22日

Outline

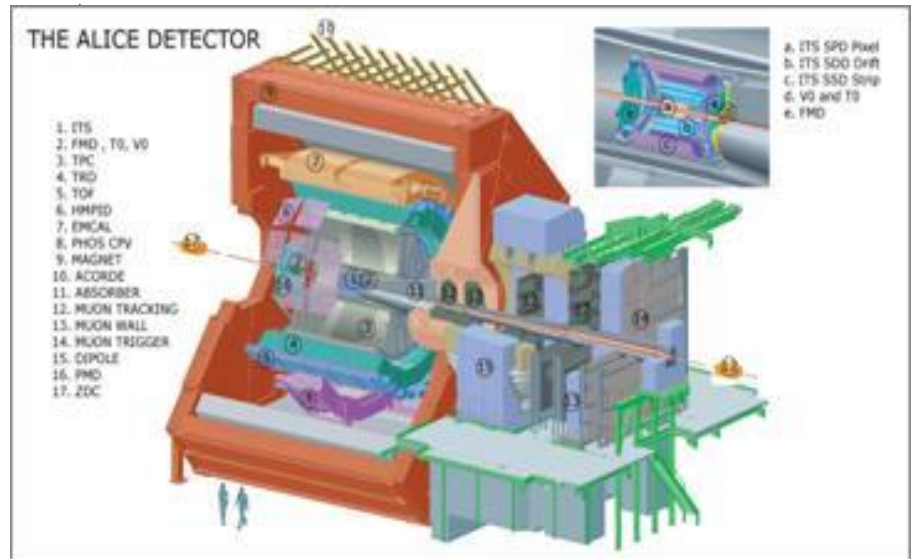
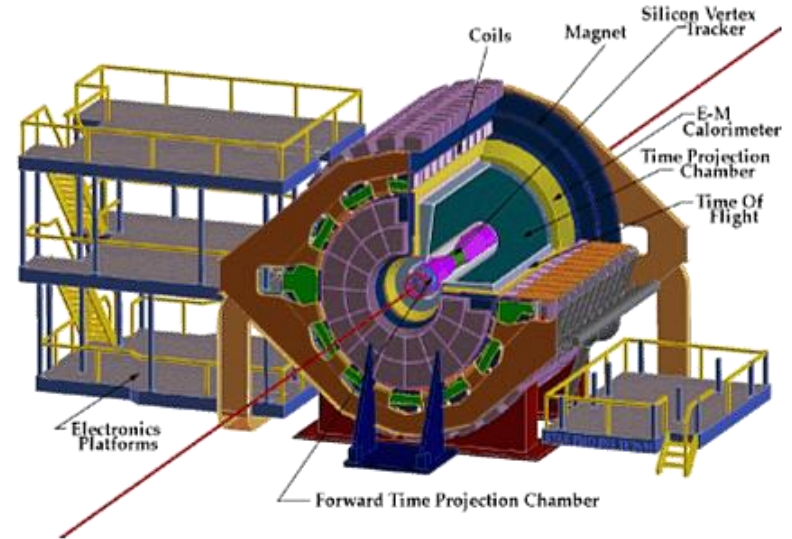
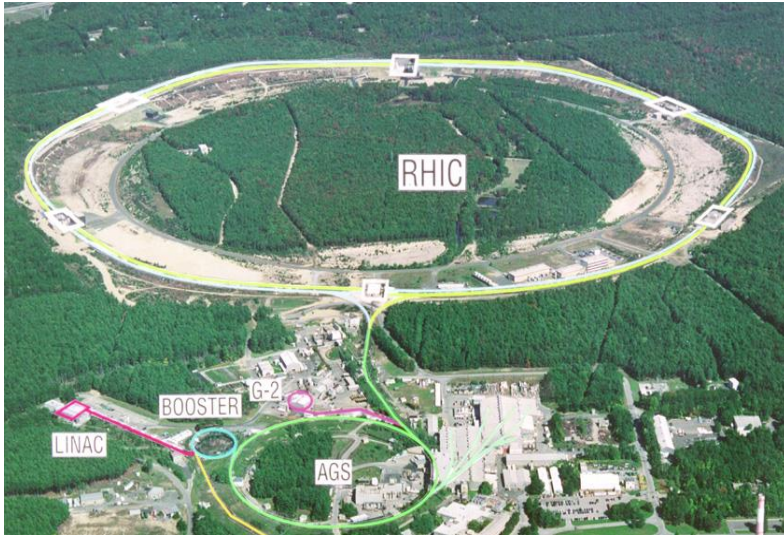
- **Introduction**
- **Flow and bulk properties (soft probes)**
 - Particle yields, spectra, flow, fluctuations, correlations, decorrelations
- **Jets and heavy flavors (hard probes)**
 - High p_T hadrons, heavy quarks/hadrons, full jets
- **Jets and flow in small collision systems**
- **Summary**

Strong-interaction QCD matter



- Low T & $\mu_B \Rightarrow$ hadrons (**hadron matter**)
- $T_c = 155 \text{ MeV} \Rightarrow$ hadron matter melts into **quark-gluon plasma**
- Very high $T \Rightarrow$ **early Universe**.
- QGP can be obtained by colliding two nuclei at extremely high energies (**relativistic heavy-ion collisions**)
- As E_{cm} increases, S increases, N_B is unchanged, S/N_B , s/n_B & T/μ_B increase

Relativistic heavy-ion collisions



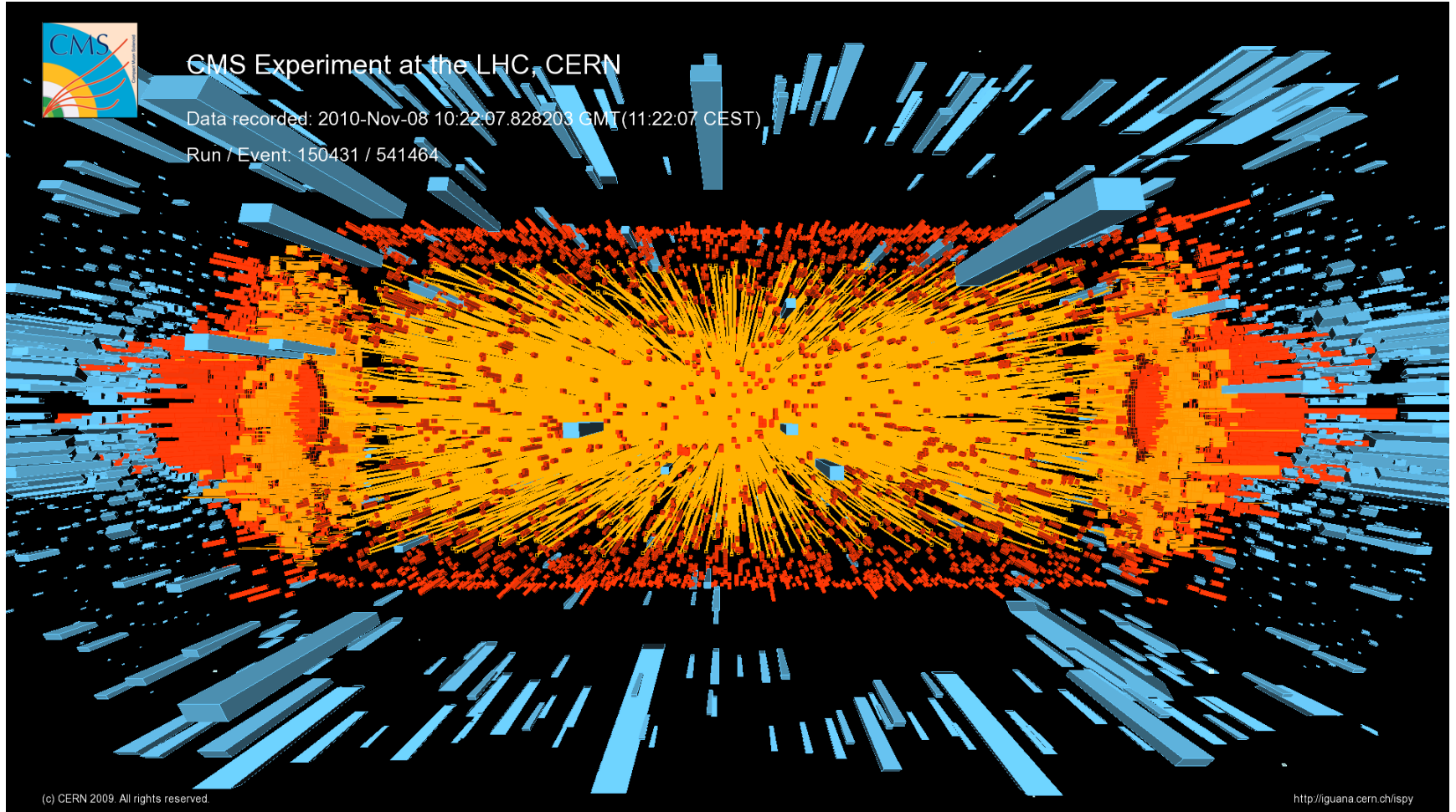
A Relativistic-Heavy Ion Collision



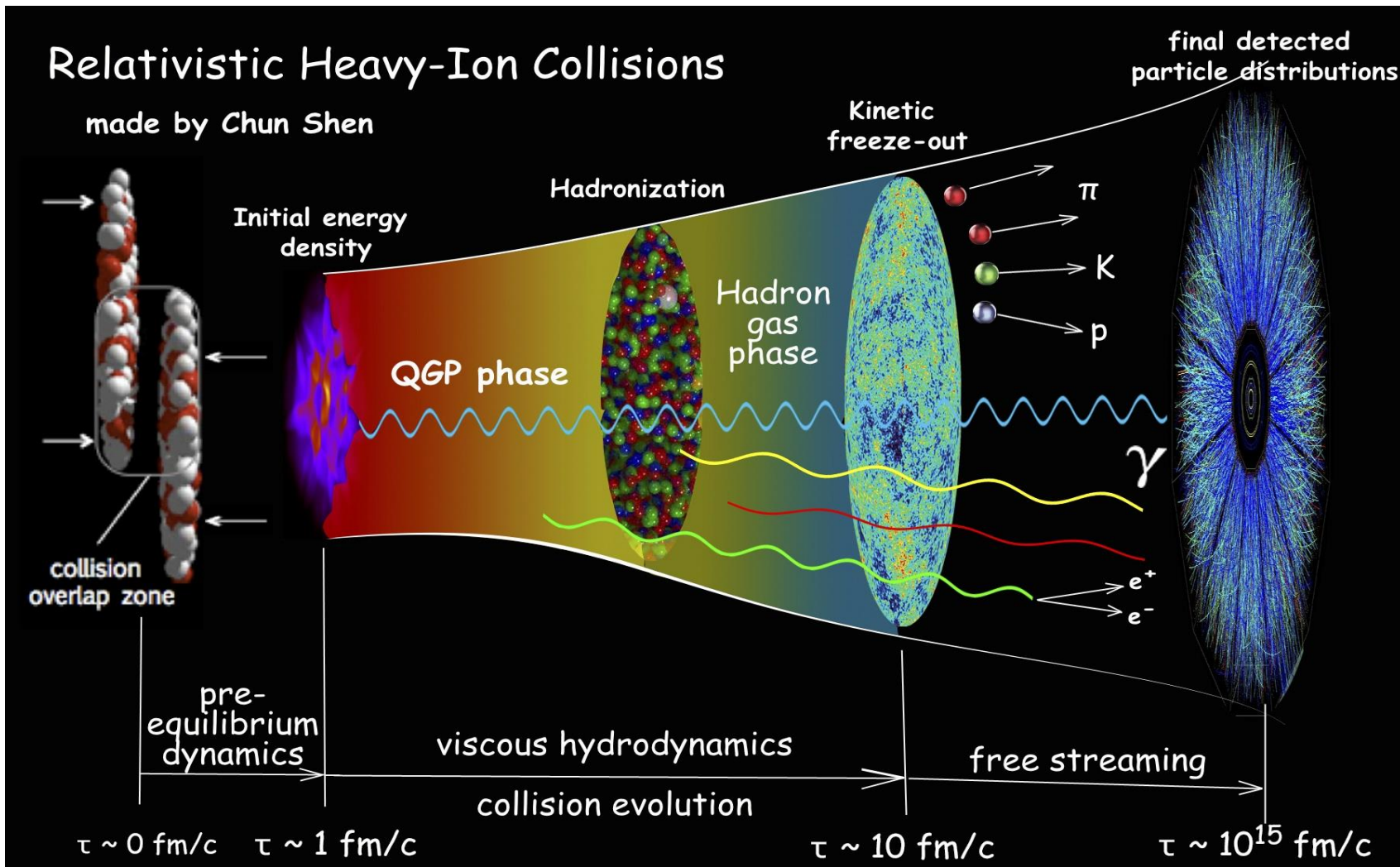
CMS Experiment at the LHC, CERN

Data recorded: 2010-Nov-08 10:22:07.828203 GMT (11:22:07 CEST)

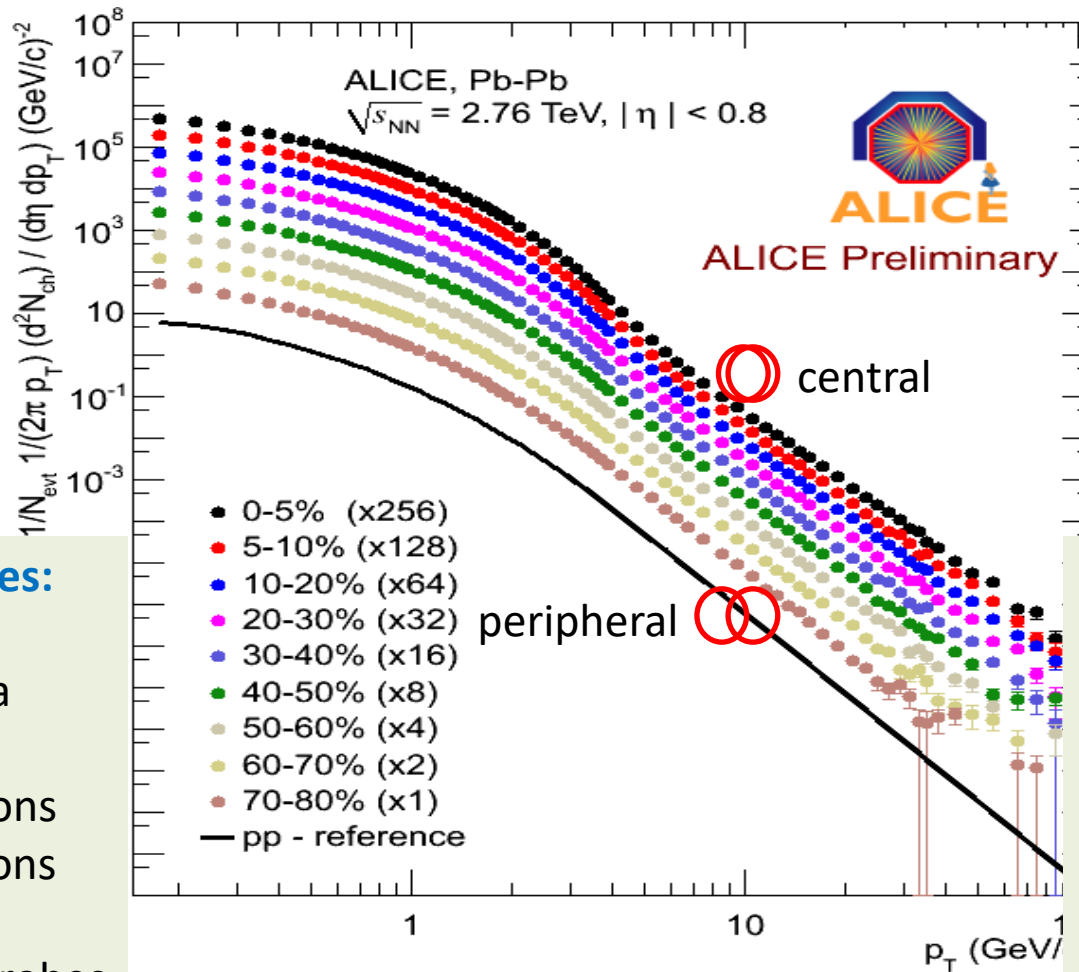
Run / Event: 150431 / 541464



“Standard Model” of RHIC & LHC heavy-ion collisions (Little Bangs)



Probes of QGP in heavy-ion collisions



Soft Probes:

Yields

Spectra

Flows

Fluctuations

Correlations

...

“Internal” probes

Hard Probes:

Jets

Large p_T hadrons

Heavy quark/hadrons

EM probes

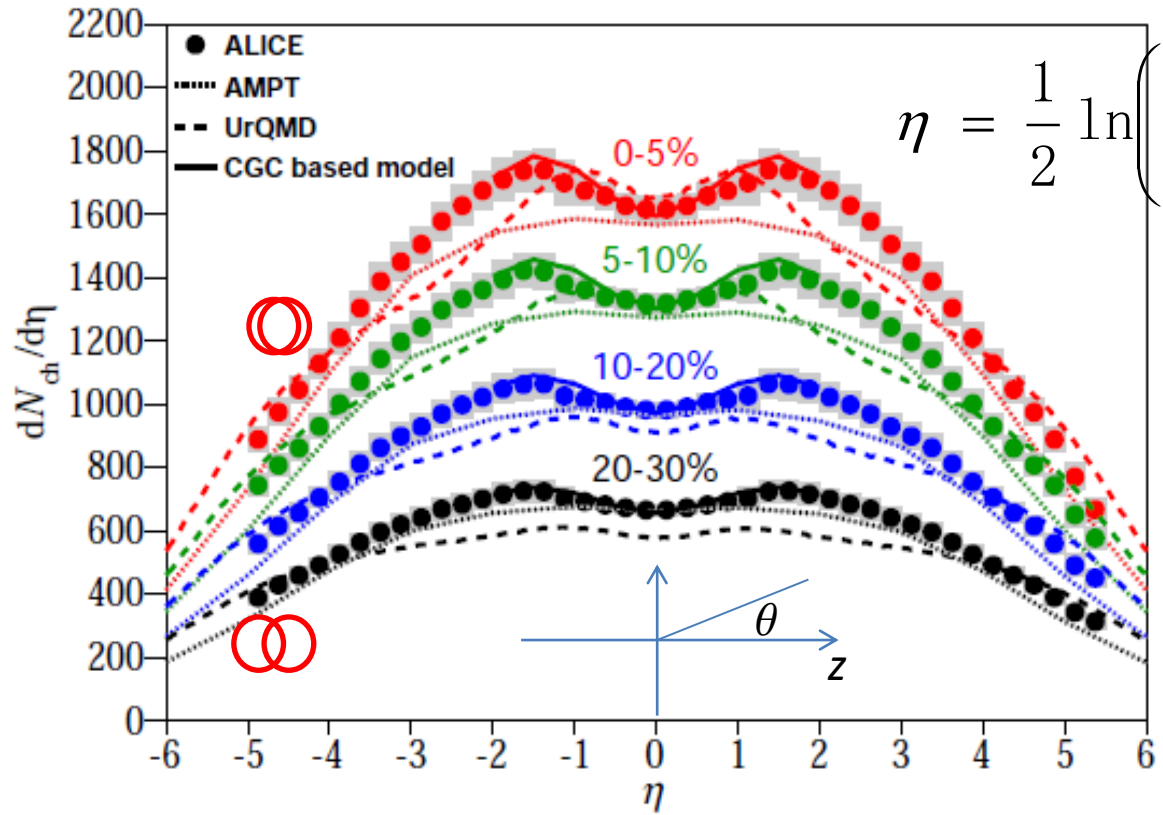
Quarkonia

...

“External” probes

Soft Probes: Flow and bulk properties

Particle distribution in longitudinal direction



$$\eta = \frac{1}{2} \ln \left(\frac{p + p_z}{p - p_z} \right) = -\ln \left(\tanh \frac{\theta}{2} \right)$$

$$LHC : \frac{dN_{ch}}{d\eta} = 1600$$

$$RHIC : \frac{dN_{ch}}{d\eta} = 700$$

$$T_c = 155 MeV$$

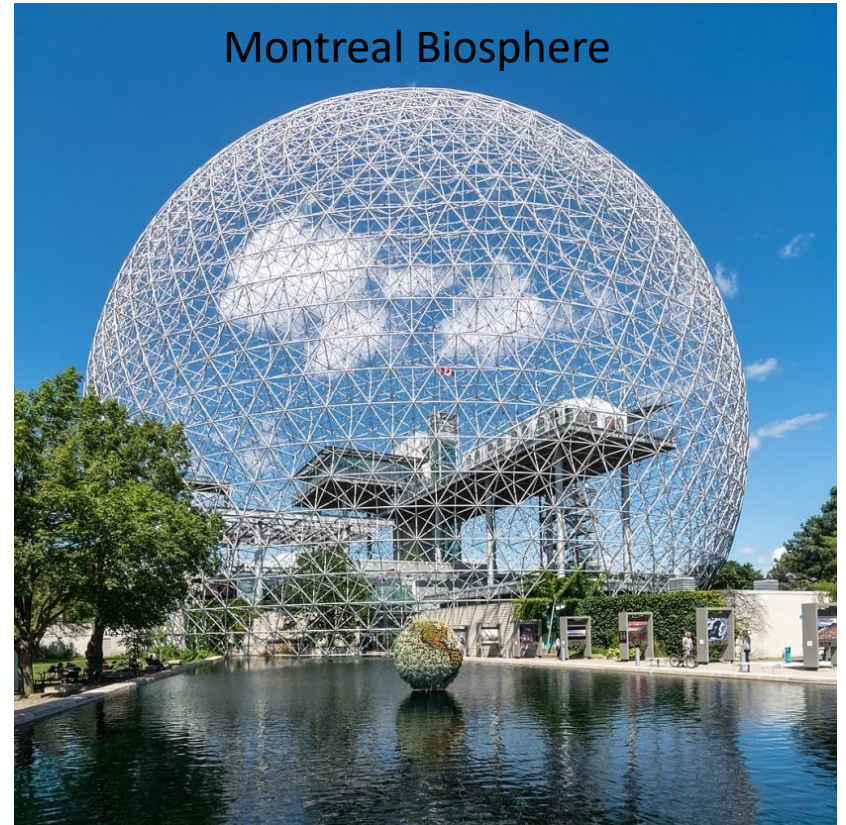
$$\varepsilon_c = 0.5 GeV / fm^3$$

$$\varepsilon_0 = \frac{dE_T}{d\eta} \frac{1}{\tau_0 \pi R^2} = \frac{3}{2} \left\langle \frac{E_T}{N} \right\rangle \frac{dN_{ch}}{d\eta} \frac{1}{\tau_0 \pi R^2}$$

$$LHC : \varepsilon_0 = 16 GeV / fm^3$$

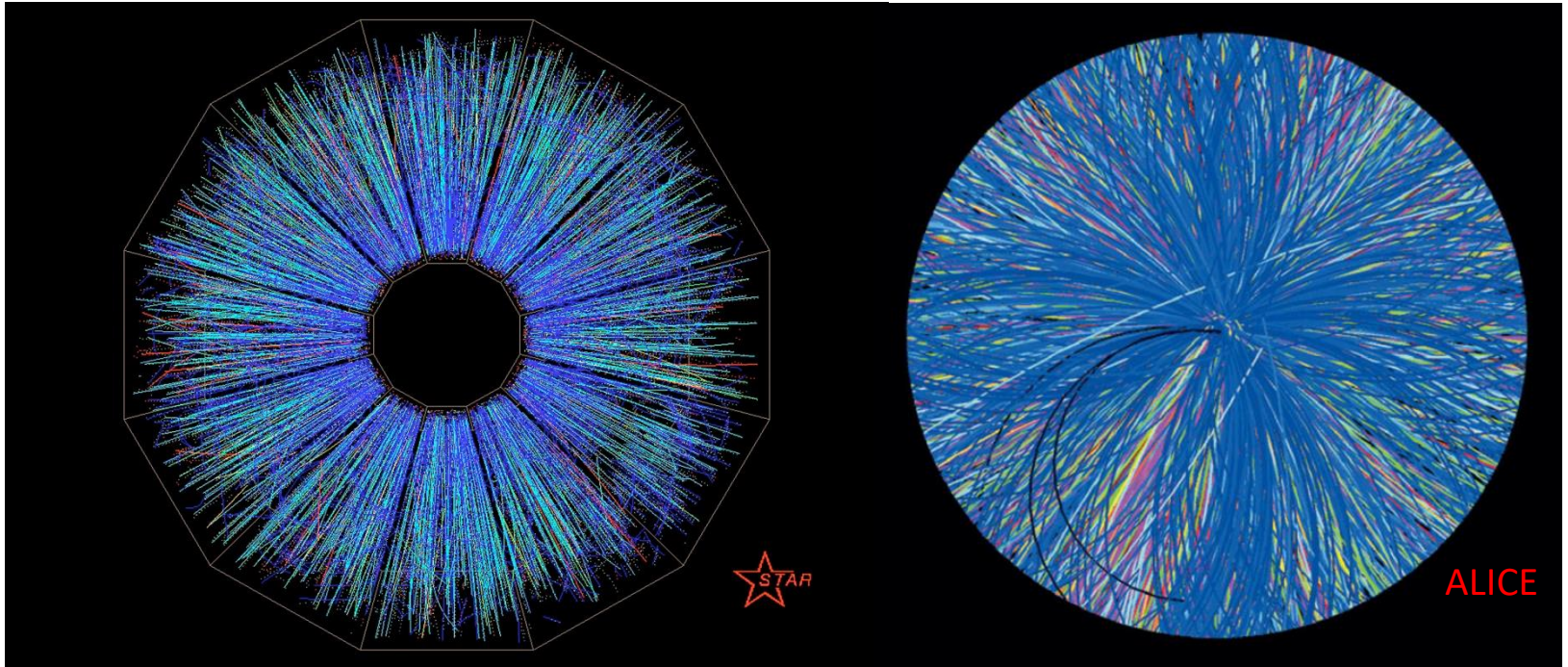
$$RHIC : \varepsilon_0 = 7 GeV / fm^3$$

How high density?



$$\frac{6 * 10^{24} \text{ kg} * (3 * 10^8 \text{ m} / \text{s})^2}{\frac{4}{3} \pi (38 \text{ m})^3} = 2.3 * 10^{36} \frac{\text{J}}{\text{m}^3} = 2.3 * 10^{36} * \frac{10^{-9} \text{ GeV} / (1.6 * 10^{-19})}{(10^{15} \text{ fm})^3} = 15 \frac{\text{GeV}}{\text{fm}^3}$$

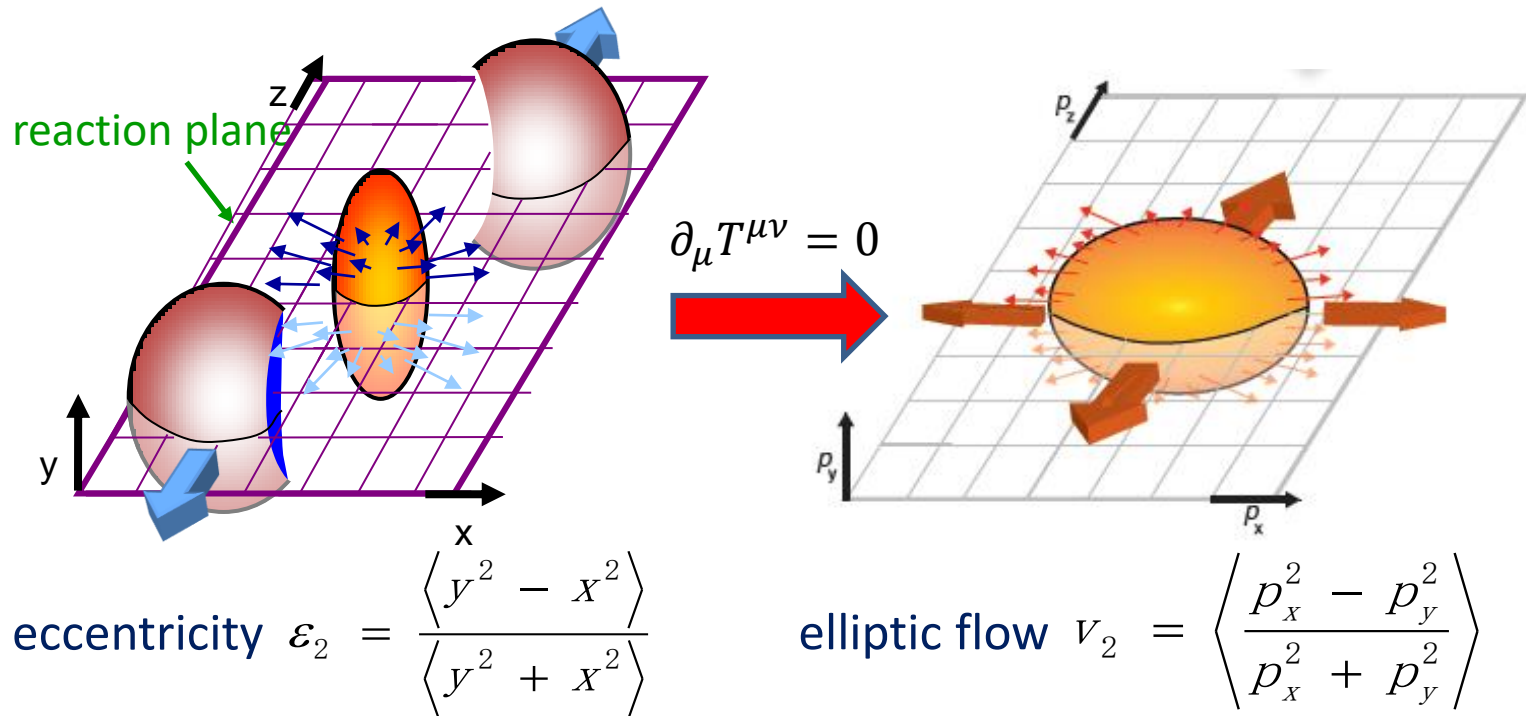
Particle distribution in transverse plane



- Particle production is not azimuthally symmetric.
- The azimuthal anisotropy can be analyzed by Fourier decomposition:

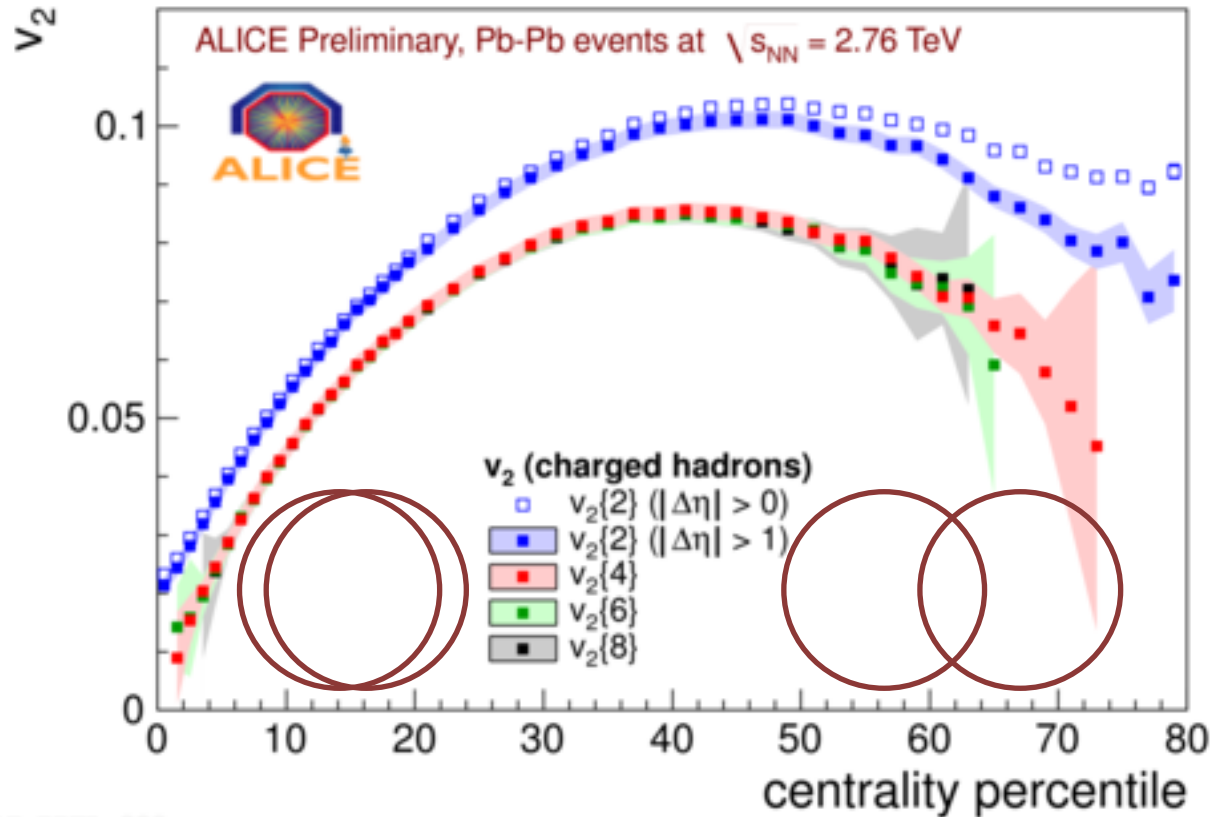
$$\frac{dN}{d\varphi} \propto 1 + \sum_n 2v_n \cos[n(\varphi - \Psi_n)]$$

Initial and final anisotropies



- The interaction among QGP constituents translates initial state geometric anisotropy to final state momentum anisotropy.

Final state anisotropy

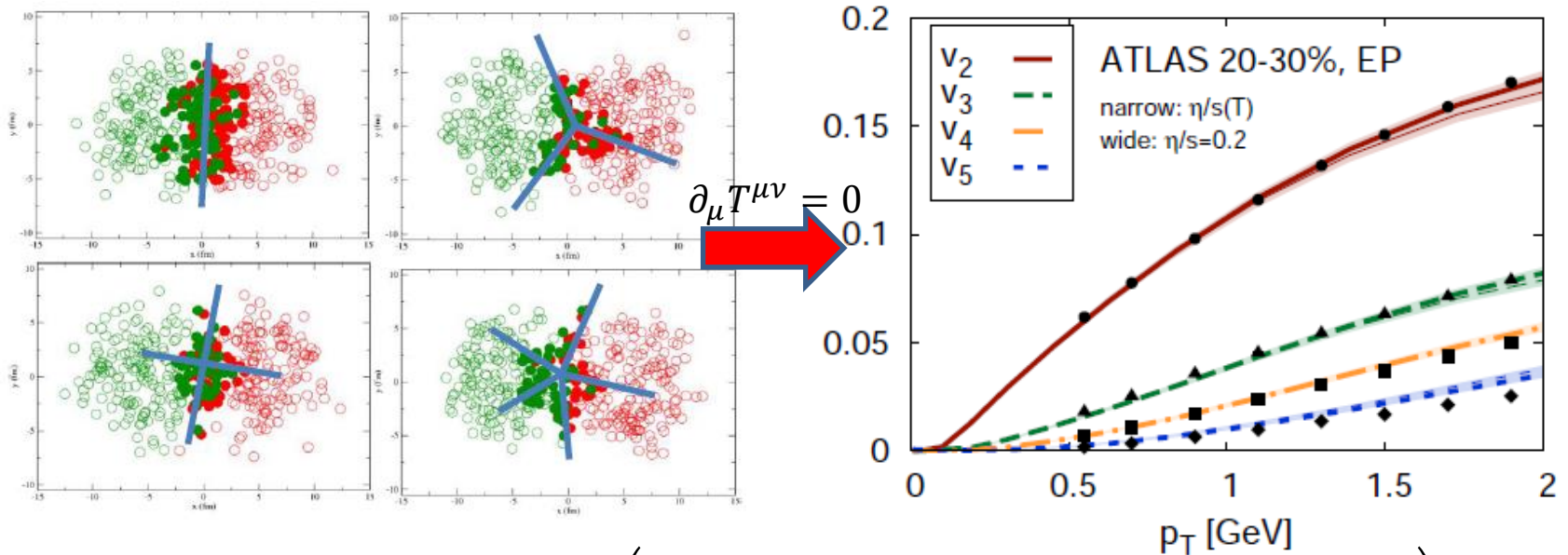


ALICE-900-900

- Strong elliptic flows depending on centrality => QGP is a strongly-coupled fluid

Initial-state fluctuations and final-state flows

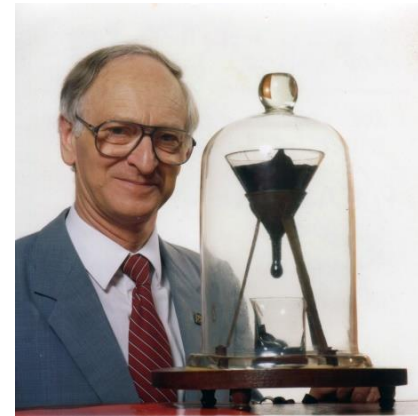
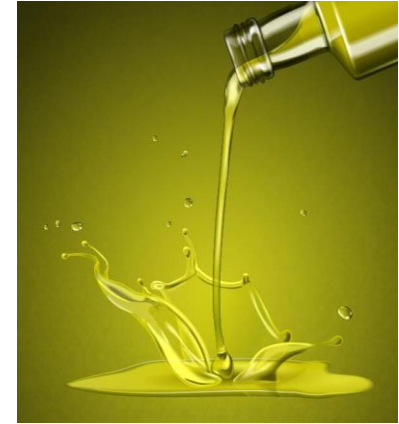
- Event-by-event initial state density and geometry fluctuations are translated into final state anisotropic flows via hydrodynamic evolution.



$$\frac{dN}{p_T dp_T dy d\phi} = \frac{dN}{2\pi p_T dp_T dy} \left(1 + \sum_n 2v_n(p_T, y) \cos\{n[\phi - \Psi_n(p_T, y)]\} \right)$$

Alver and Roland, PRC 2010; GYQ, Petersen, Bass, Muller, PRC 2010; Staig, Shuryak, PRC 2011; Teaney, Yan, PRC 2011; Gale, Jeon, Schenke, Tribedy, Venugopalan, PRL 2012; etc.

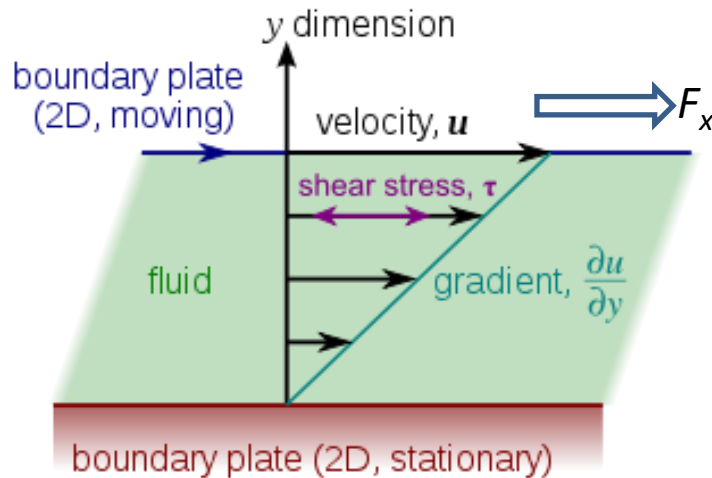
Fluidity



- How the fluid flows depends on its viscosity.

Shear viscosity

- Shear viscosity η measures the resistance to shear flow.



$$\frac{F_x}{A_y} = \eta \frac{\partial u_x}{\partial y}$$

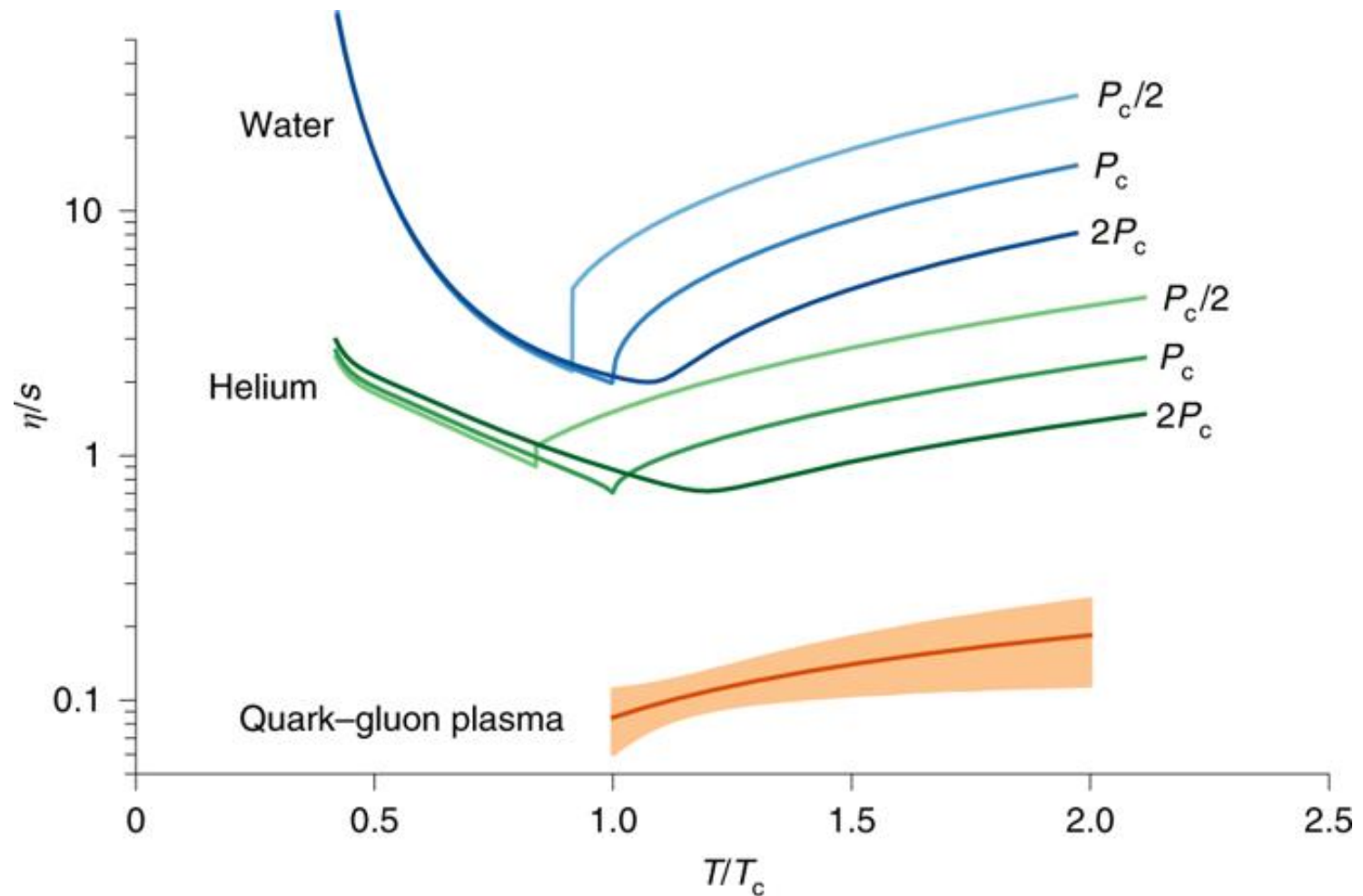
- Shear viscosity η measures the ability of momentum transport between different parts of the system.
- From kinetic theory, it is related to the strength of the interactions among the constituents of the system.

$$\eta \approx \frac{1}{3} n \lambda \bar{p}$$

一些流体的粘滞系数

流体	粘滞系数 (Pa*s)
空气	1.8×10^{-5}
水	8.9×10^{-4}
牛奶	1.8×10^{-3}
橄榄油	0.04
蜂蜜	10
花生酱	250
沥青	2×10^8
夸克胶子等离子体	???

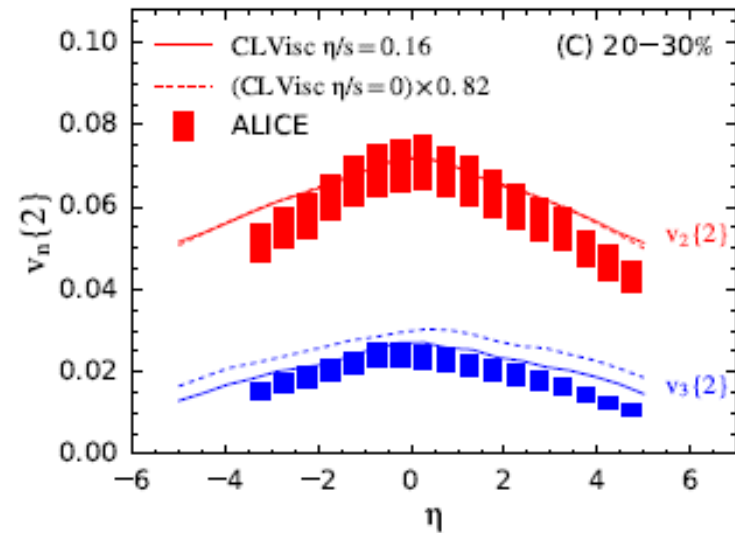
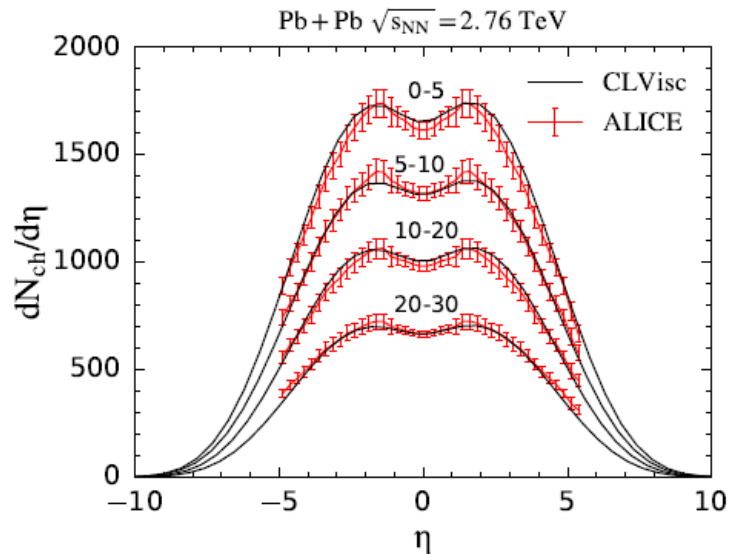
Most perfect fluid



Bernhard, Moreland, Bass, Nature Physics 2019

Longitudinal fluctuations

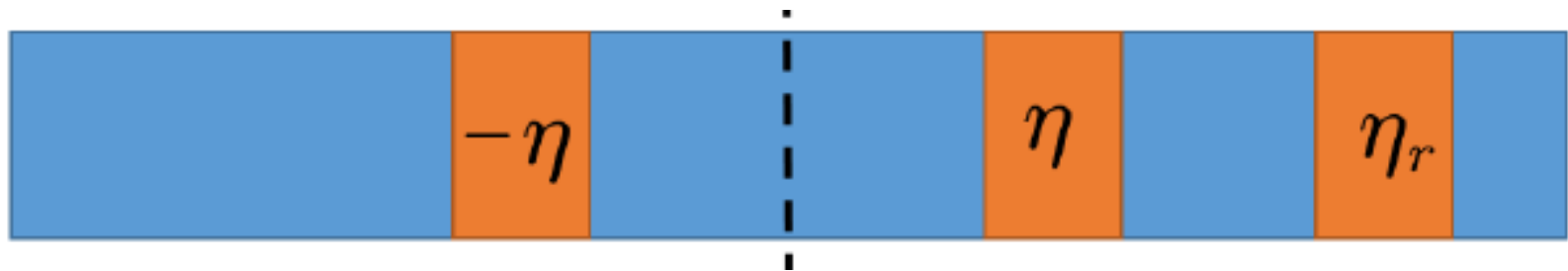
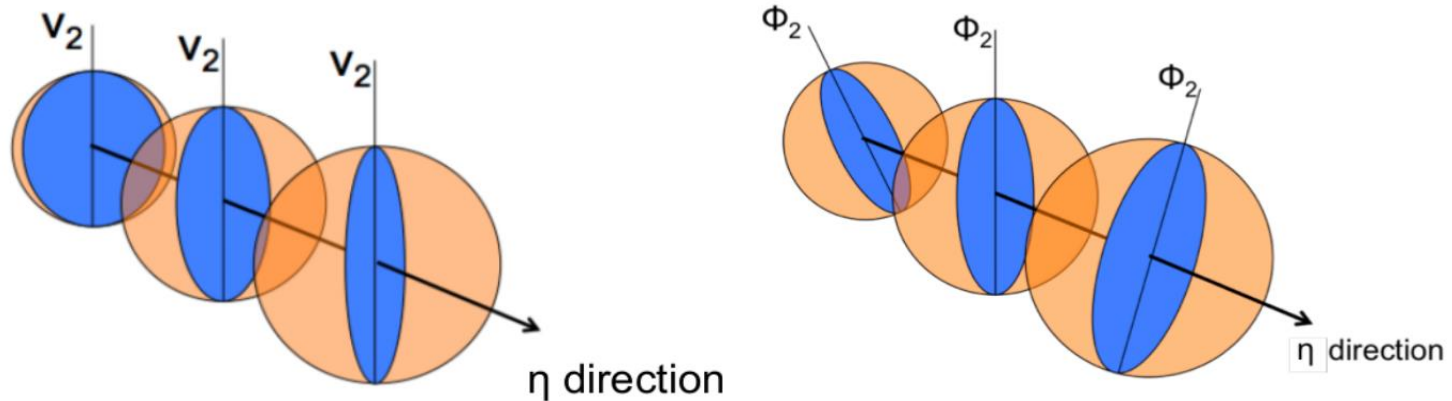
- The initial states are fluctuating also in longitudinal (rapidity) directions



- Longitudinal fluctuations can lead to rapidity-dependent particle yield and v_n
- The rapidity dependence (decorrelation) of v_n may be used to probe the QGP properties

Gabriel et al. PRL 2016; Pang, Petersen, Wang PRC 2018

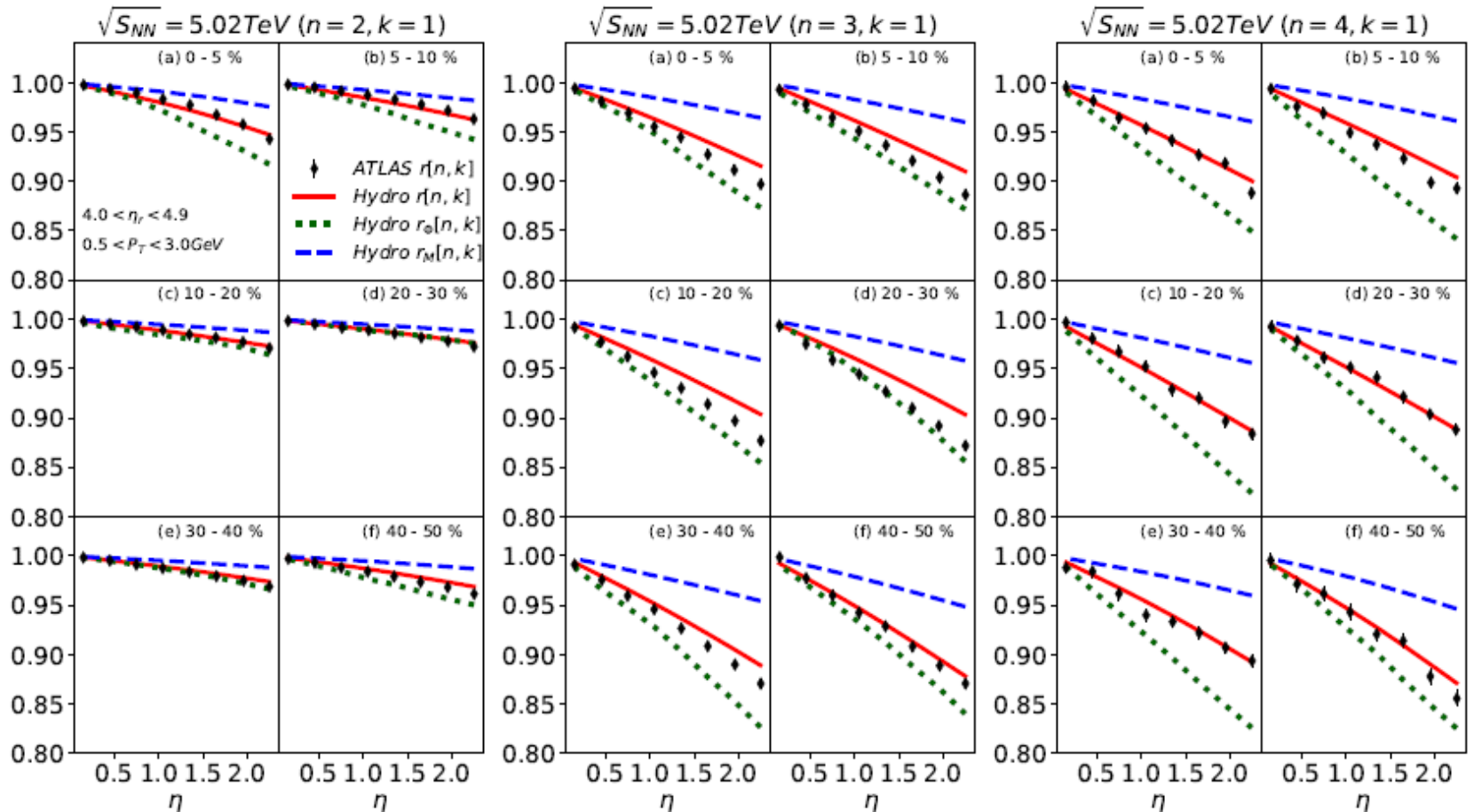
Longitudinal fluctuations and decorrelations



$$r[n, k](\eta) = \frac{\langle Q_n^k(-\eta) Q_n^{*k}(\eta_r) \rangle}{\langle Q_n^k(\eta) Q_n^{*k}(\eta_r) \rangle}$$

Petersen, Bhattacharya, Bass, Greiner, PRC 2011; Xiao, Liu, Wang, PRC 2013; Pang, GYQ, Roy, Wang, Ma, PRC 2015; Pang, Petersen, GYQ, Roy, Wang, EPJA 2016; Jia, Huo, PRC 2014; CMS, PRC 2015; Jia et al, JPG 2017; ATLAS EPJC 2018; Bozek, Broniowski, PRC 2018; Wu, Pang, GYQ, Wang, PRC 2018; etc.

Longitudinal fluctuations and decorrelations

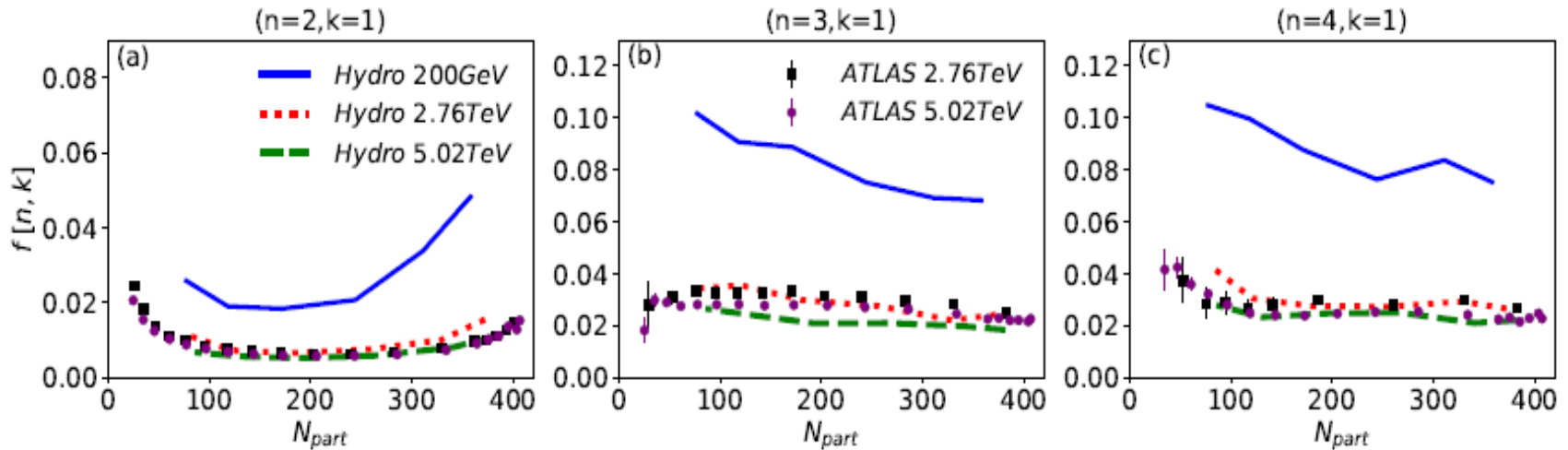


$$r[n, k](\eta) = \frac{\langle Q_n^k(-\eta) Q_n^{*k}(\eta_r) \rangle}{\langle Q_n^k(\eta) Q_n^{*k}(\eta_r) \rangle}$$

$$r[n, k](\eta) \approx 1 - 2f[n, k]\eta$$

Pang, GYQ, Roy, Wang, Ma, PRC 2015; Pang, Petersen, GYQ, Roy, Wang, EPJA 2016;
 Wu, Pang, GYQ, Wang, PRC 2018

Longitudinal fluctuations and decorrelations



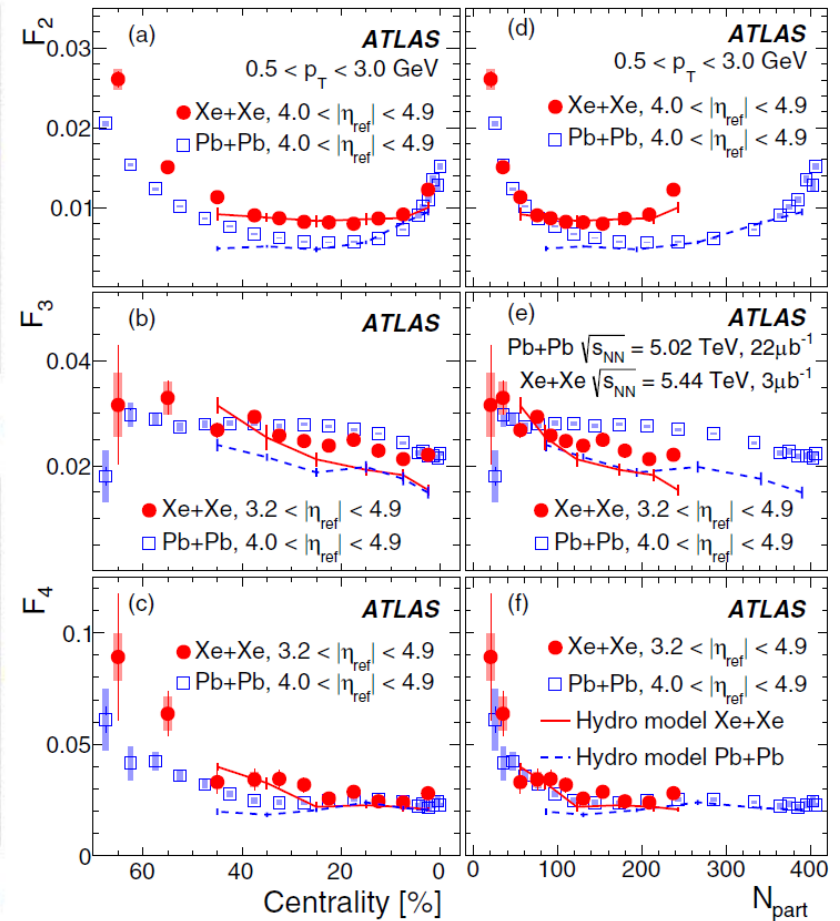
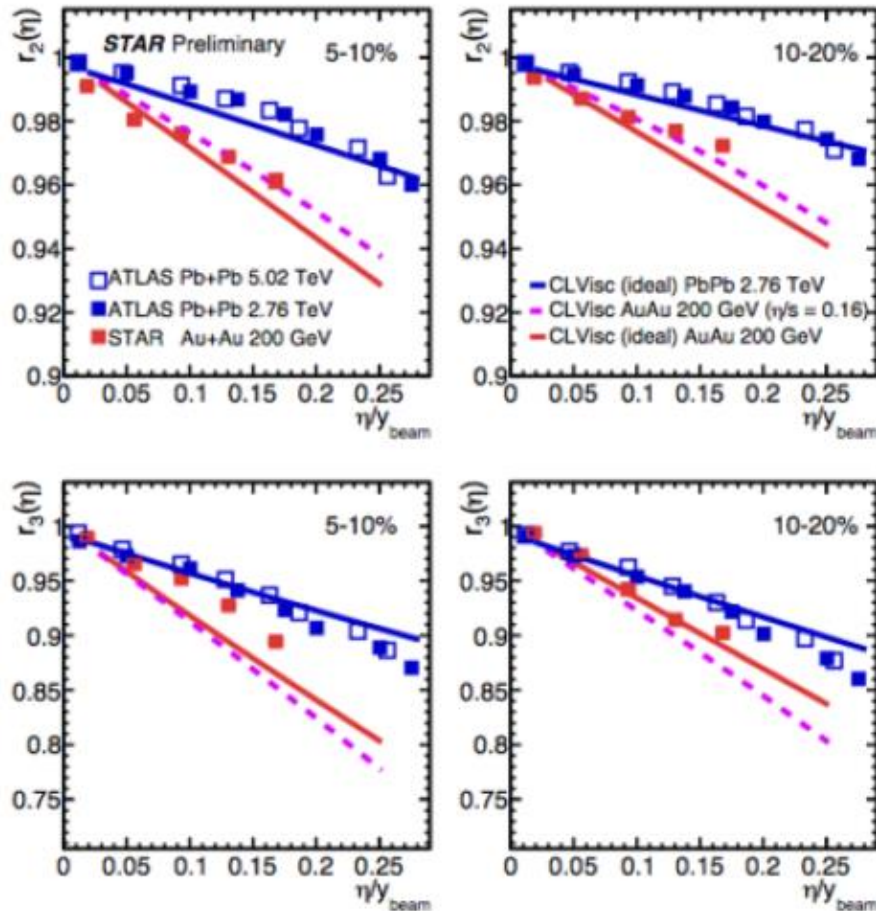
$$r[n, k](\eta) \approx 1 - 2f[n, k]\eta$$

$$f[n, k] = \frac{\sum_i \{1 - r[n, k](\eta_i)\} \eta_i}{2 \sum_i \eta_i^2}$$

- Decorrelation effects: $f[200\text{GeV}] > f[2.76\text{TeV}] > f[5.02\text{TeV}]$
- For v_2 , non-monotonic centrality dependence due to initial collision geometry.
- For v_3 & v_4 , weak centrality dependence, slight increase of decorrelation effects from central to peripheral collisions.

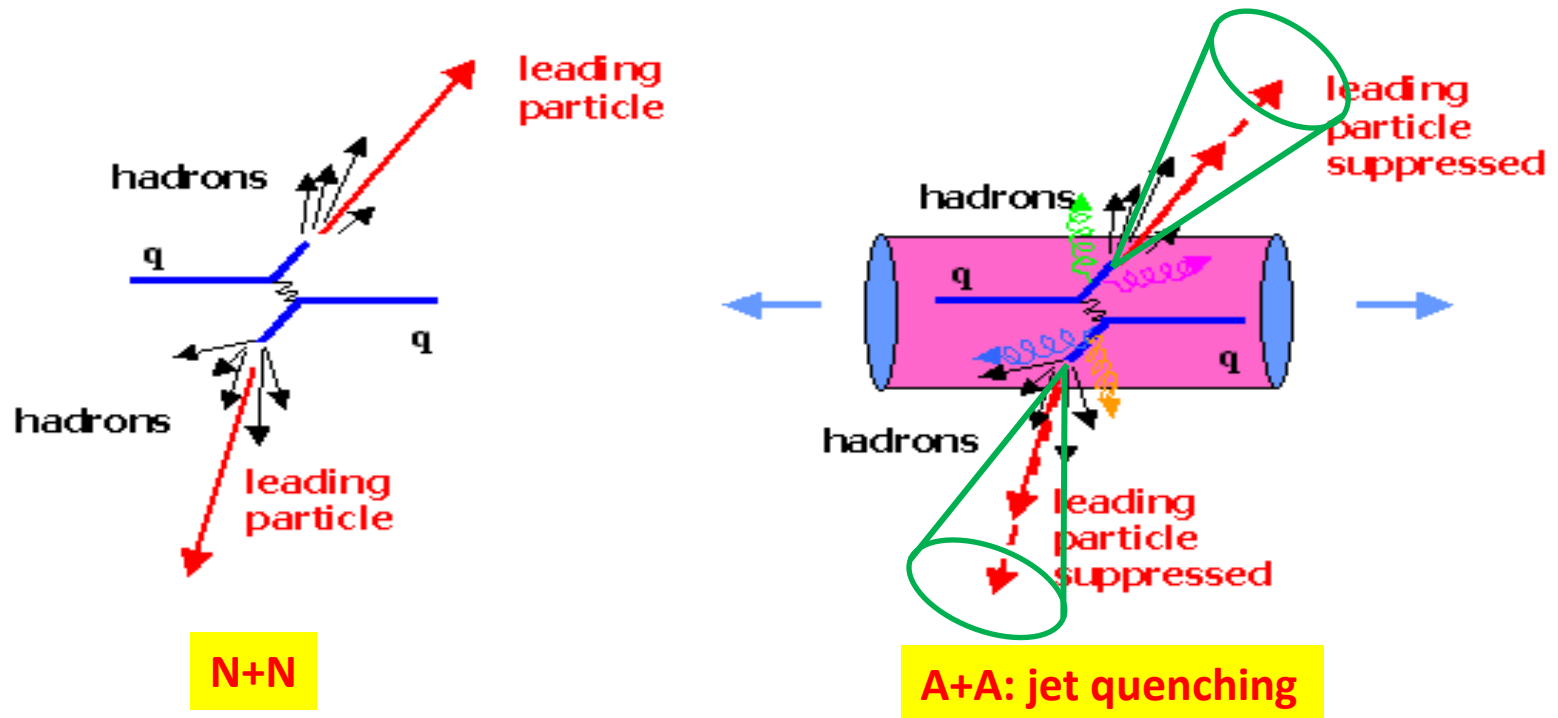
Pang, GYQ, Roy, Wang, Ma, PRC 2015; Pang, Petersen, GYQ, Roy, Wang, EPJA 2016;
Wu, Pang, GYQ, Wang, PRC 2018

Longitudinal decorrelations in different collision energies and systems



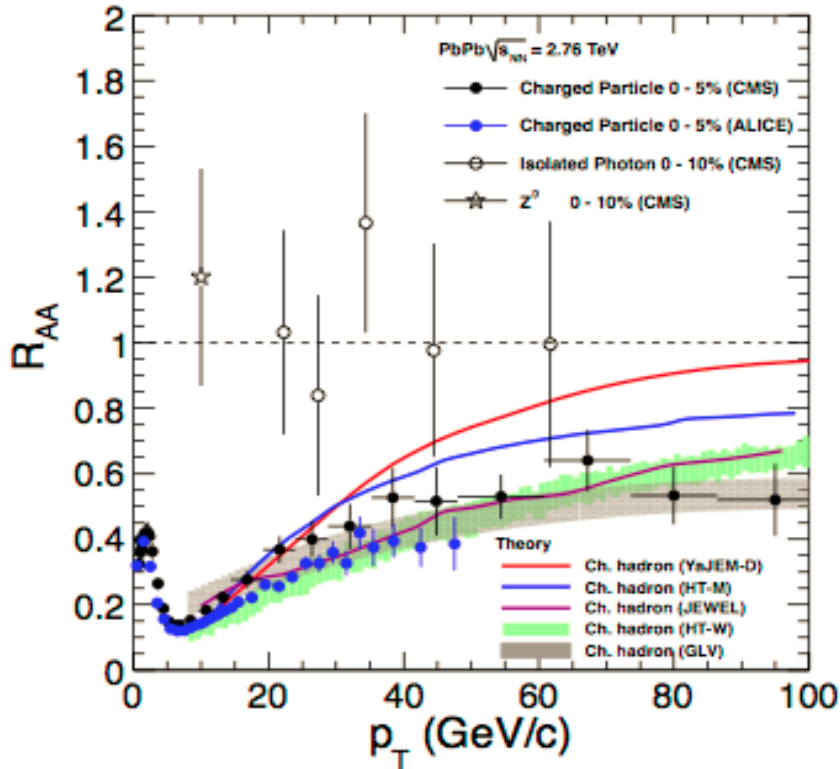
Hard Probes: Jets and heavy flavors

Jet quenching

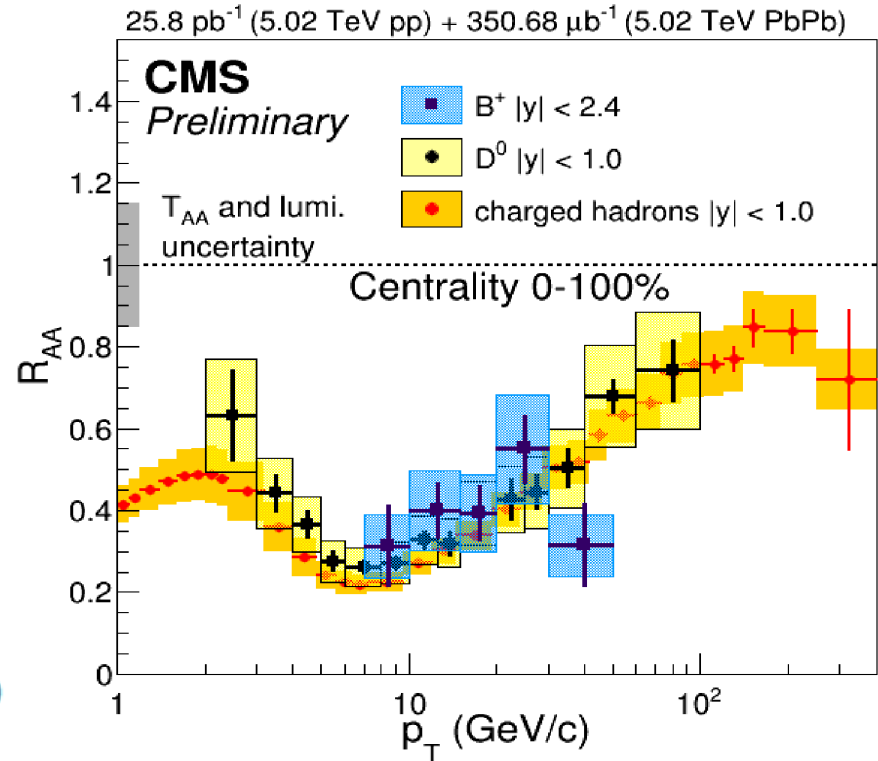


- Jets and jet-medium interaction (jet quenching) provide valuable tools to probe hot & dense QGP in heavy-ion collisions (at RHIC & LHC):
- (1) jet energy loss (2) jet deflection and broadening (3) modification of jet structure/substructure (4) jet-induced medium excitation

Nuclear modifications of large p_T hadrons

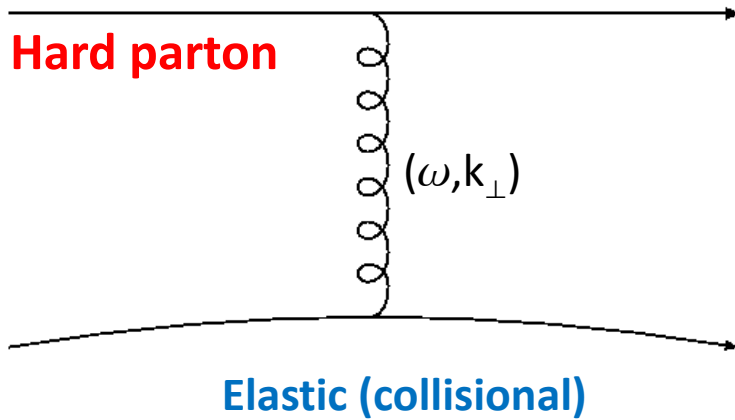


$$R_{AA} = \frac{1}{N_{coll}} \frac{dN^{AA} / d^2 p_T dy}{dN^{pp} / d^2 p_T dy}$$



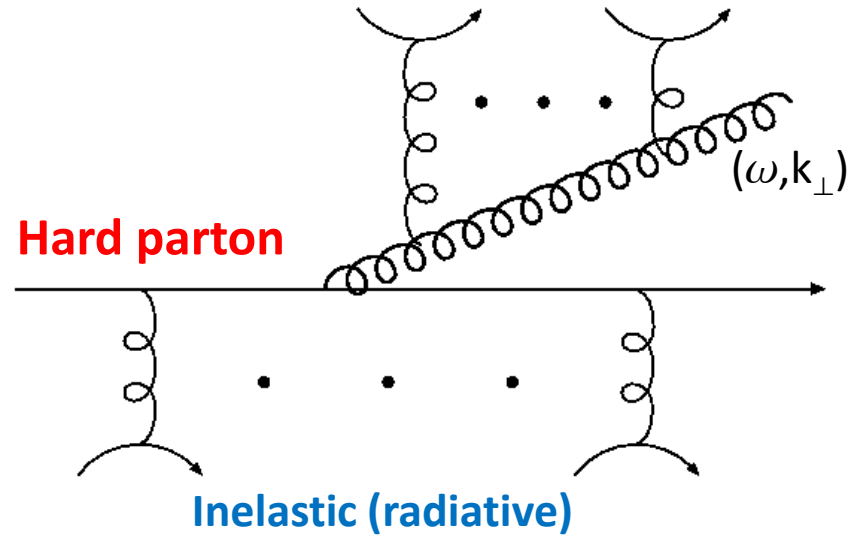
Color & flavor dependences of parton energy loss: $\Delta E_g > \Delta E_{uds} > \Delta E_c > \Delta E_b$?

Elastic and inelastic interactions



$$\frac{d\Gamma_{coll}}{d\omega dk_{\perp}^2 dt}(T, E, \dots) = ?$$

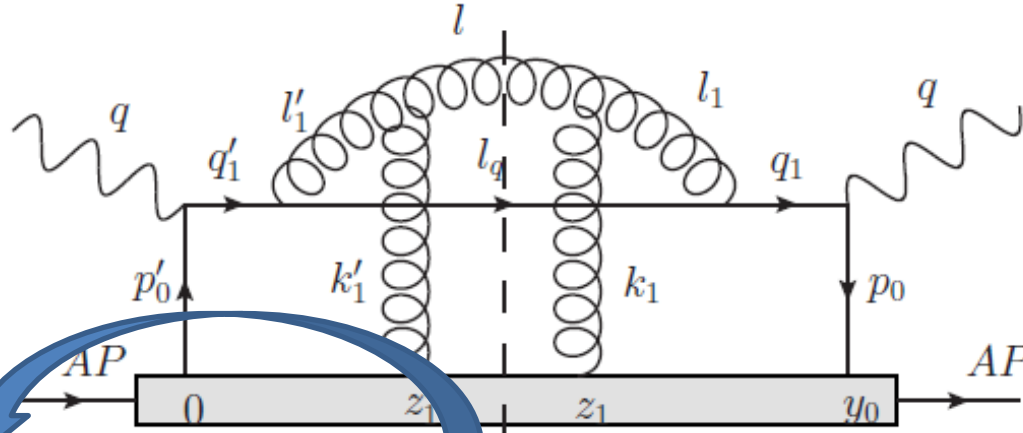
Bjorken 1982; Bratten, Thoma 1991; Thoma, Gyulassy, 1991; Mustafa, Thoma 2005; Peigne, Peshier, 2006; Djordjevic, 2006; Wicks et al (DGLV), 2007; GYQ et al (AMY), 2008; ...



$$\frac{d\Gamma_{rad}}{d\omega dk_{\perp}^2 dt}(T, E, \dots) = ?$$

BDMPS-Z: Baier-Dokshitzer-Mueller-Peigne-Schiff-Zakharov
ASW: Amesto-Salgado-Wiedemann
AMY: Arnold-Moore-Yaffe (& Caron-Huot, Gale)
GLV: Gyulassy-Levai-Vitev (& Djordjevic, Heinz)
HT: Wang-Guo (& Zhang, Wang, Majumder)

Medium-induced inelastic (radiative) process



Zhang, Hou, GYQ, PRC 2018
& PRC 2019; Zhang, GYQ,
Wang, PRD 2019.

+ other 20 diagrams

$$\begin{aligned}
 \frac{dN_g^{med}}{dy d^2\mathbf{1}_\perp} &= \frac{\alpha_s}{2\pi^2} P(y) \int dZ_1^- \int \frac{dk^- d^2\mathbf{k}_{1\perp}}{(2\pi)^3} \mathcal{D}(k_1^-, \mathbf{k}_{1\perp}) \\
 &\times \left\{ \left[2 - 2 \cos \left(\frac{y(1-y)}{(y-\lambda_1^-)(1+\lambda_1^- - y)} \frac{(\mathbf{1}_\perp - \mathbf{k}_{1\perp})^2 + (y-\lambda_1^-)^2 M^2}{l_1^2 + y^2 M^2} \frac{Z_1^-}{\tilde{\tau}_{form}^-} \right) \right] \right. \\
 &C_A \left[\frac{1 + (1 + \lambda_1^- - y)^2}{1 + (1 - y)^2} \left(\frac{y - \frac{\lambda_1^-}{2}}{y - \lambda_1^-} \right)^2 \frac{(\mathbf{1}_\perp - \mathbf{k}_{1\perp})^2 + \frac{(y-\lambda_1^-)^4 M^2}{1+(1+\lambda_1^- - y)^2}}{[(\mathbf{1}_\perp - \mathbf{k}_{1\perp})^2 + (y - \lambda_1^-)^2 M^2]^2} \right. \\
 &- \frac{1 + (1 + \lambda_1^- - y)(1 - y)}{2[1 + (1 - y)^2]} \left(\frac{y - \frac{\lambda_1^-}{2}}{y - \lambda_1^-} \right) \frac{\mathbf{1}_\perp \cdot (\mathbf{1}_\perp - \mathbf{k}_{1\perp}) + \frac{y^2(y-\lambda_1^-)^2}{1+(1+\lambda_1^- - y)(1-y)} M^2}{[l_1^2 + y^2 M^2] [(\mathbf{1}_\perp - \mathbf{k}_{1\perp})^2 + (y - \lambda_1^-)^2 M^2]} \\
 &\left. \left. - \frac{1 + (1 + \lambda_1^- - y)(1 - \frac{y}{1+\lambda_1^-})}{2[1 + (1 - y)^2]} \left(\frac{y - \frac{\lambda_1^-}{2}}{y - \lambda_1^-} \right) \frac{(\mathbf{1}_\perp - \mathbf{k}_{1\perp}) \cdot \left(\mathbf{1}_\perp - \frac{y}{1+\lambda_1^-} \mathbf{k}_{1\perp} \right) + \frac{\left(\frac{y}{1+\lambda_1^-} \right)^2 (y-\lambda_1^-)^2}{1+(1+\lambda_1^- - y)(1 - \frac{y}{1+\lambda_1^-})} M^2}{\left[\left(\mathbf{1}_\perp - \frac{y}{1+\lambda_1^-} \mathbf{k}_{1\perp} \right)^2 + \left(\frac{y}{1+\lambda_1^-} \right)^2 M^2 \right] [(\mathbf{1}_\perp - \mathbf{k}_{1\perp})^2 + (y - \lambda_1^-)^2 M^2]} \right] + \dots \right\}
 \end{aligned}$$

Medium-induced gluon emission beyond collinear expansion & soft emission limit with transverse & longitudinal scatterings for massive/massless quarks

Linearized Boltzmann Transport (LBT) Model

- Boltzmann equation:** $p_1 \cdot \partial f_1(x_1, p_1) = E_1 C [f_1]$

- Elastic collisions:**

$$\Gamma_{12 \rightarrow 34} = \frac{\gamma_2}{2E_1} \int \frac{d^3 p_2}{(2\pi)^3 2E_2} \int \frac{d^3 p_3}{(2\pi)^3 2E_3} \int \frac{d^3 p_4}{(2\pi)^3 2E_4}$$

$$\times f_2(\vec{p}_2) \left[1 \pm f_3(\vec{p}_1 - \vec{k}) \right] \left[1 \pm f_4(\vec{p}_2 + \vec{k}) \right]$$

$$\times (2\pi)^4 \delta^{(4)}(p_1 + p_2 - p_3 - p_4) |\mathcal{M}_{12 \rightarrow 34}|^2$$

$$P_{el} = 1 - e^{-\Gamma_{el} \Delta t} \quad \text{Matrix elements taken from LO pQCD}$$

- Inelastic collisions:**

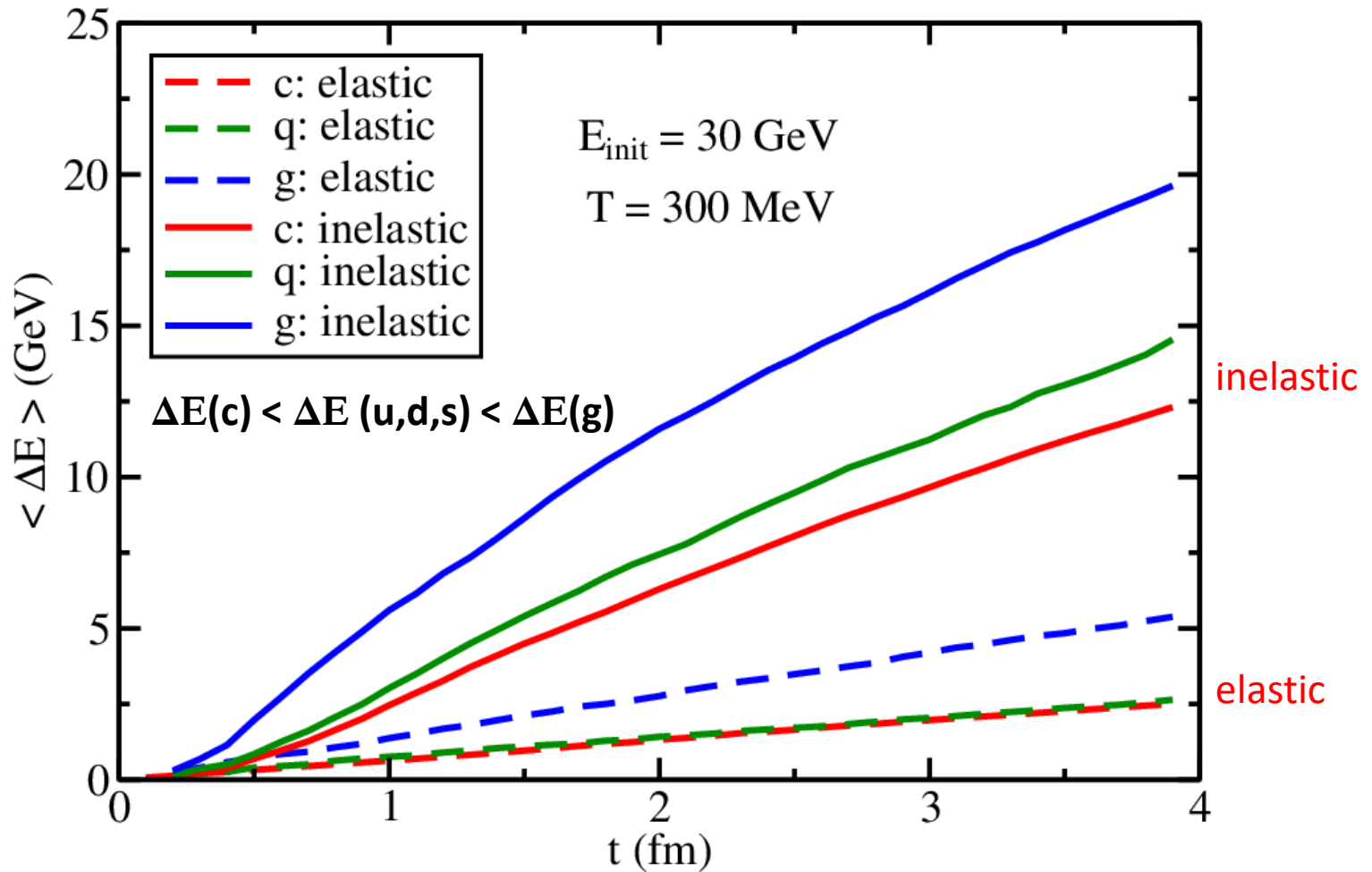
$$\langle N_g \rangle = \Gamma_g \Delta t = \Delta t \int dx dk_{\perp}^2 \frac{dN_g}{dx dk_{\perp}^2 dt}$$

$$P_{inel} = 1 - e^{-\langle N_g \rangle} \quad \text{Radiation spectra taken from Guo, Wang PRL 2000; Zhang, Wang, Wang 2004}$$

- Elastic + Inelastic:** $P_{tot} = 1 - e^{-\Gamma_{tot} \Delta t} = P_{el} + P_{inel} - P_{el} P_{inel}$

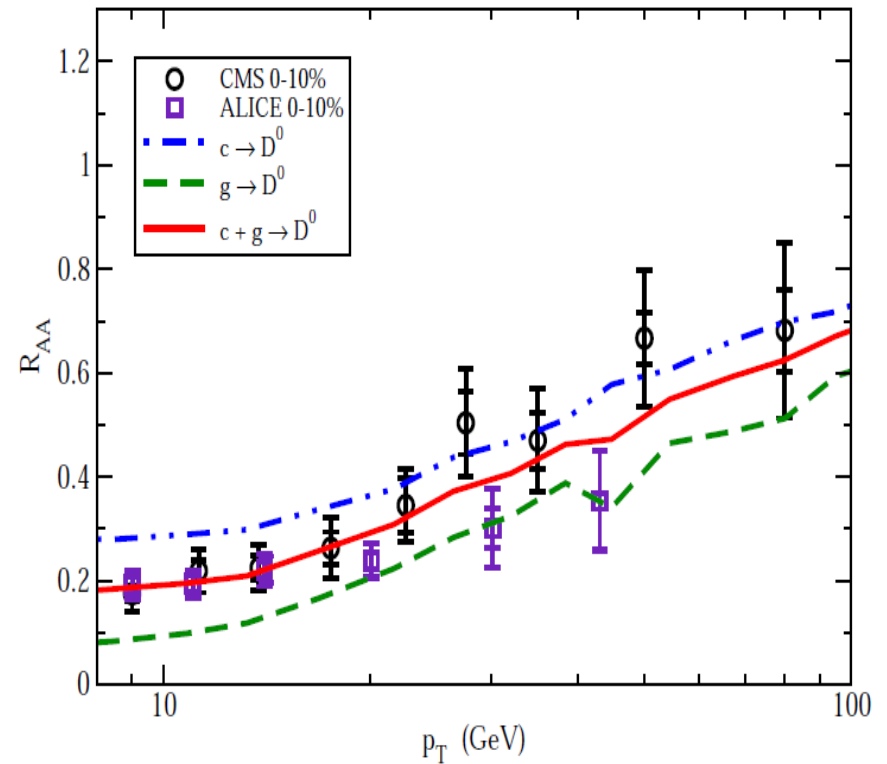
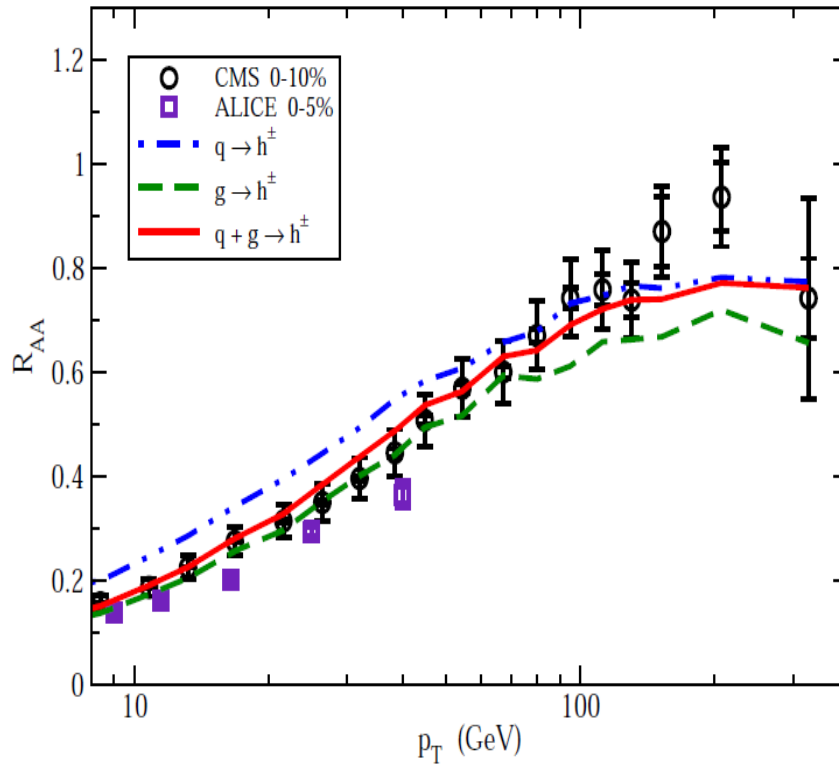
He, Luo, Wang, Zhu, PRC 2015; Cao, Luo, GYQ, Wang, PRC 2016, PLB 2018; etc.

Parton energy loss in LBT



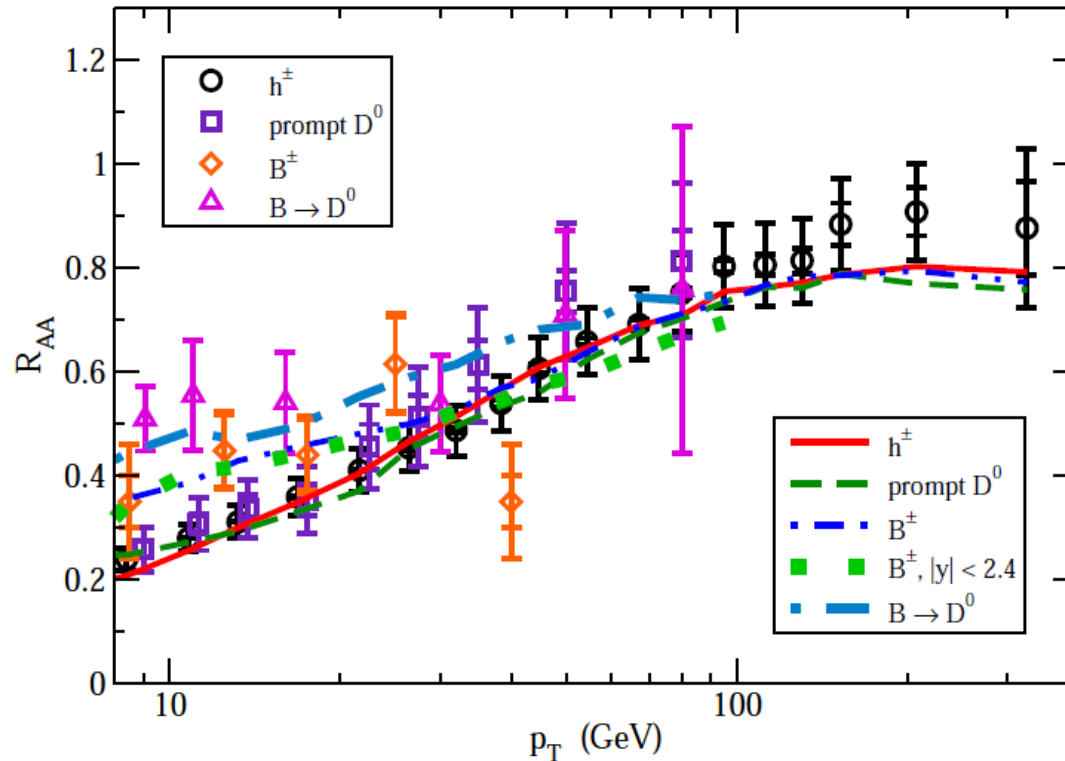
He, Luo, Wang, Zhu, PRC 2015; Cao, Luo, GYQ, Wang, PRC 2016 ; PLB 2018; etc.

Charged hadron & D meson R_{AA}



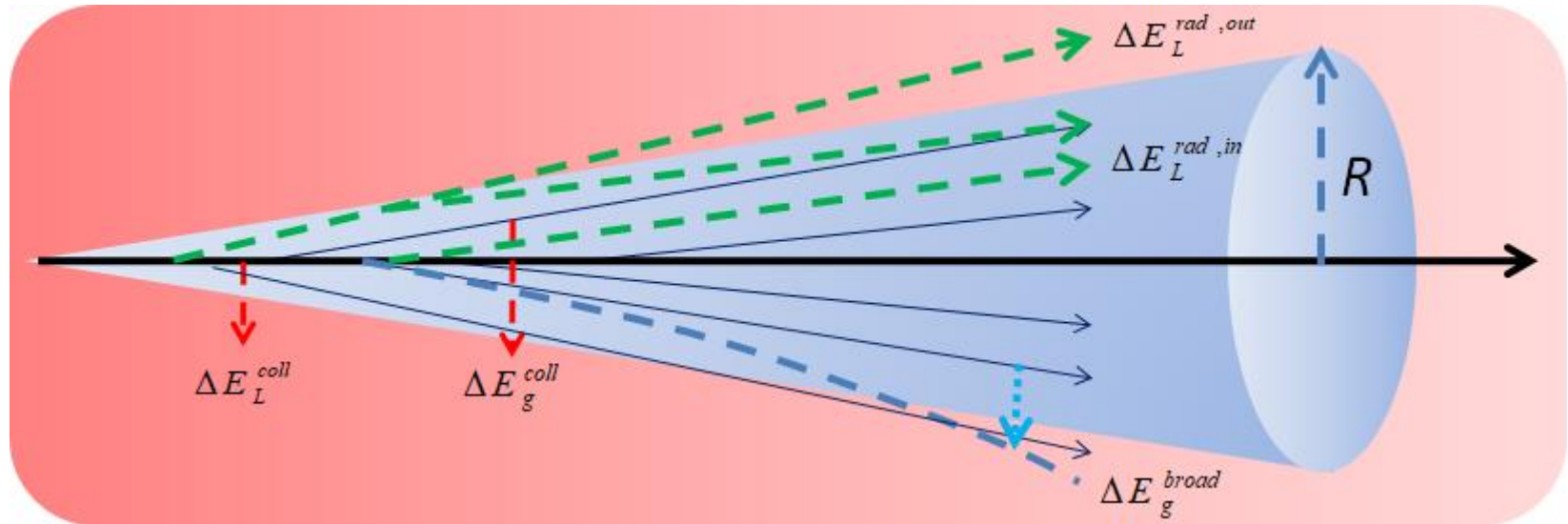
- A state-of-art jet quenching framework (NLO-pQCD + LBT + Hydrodynamics)
- Quark-initiated hadrons have less quenching effects than gluon-initiated hadrons.
- Combining both quark and gluon contributions, we obtain a nice description of charged hadron & D meson R_{AA} over a wide range of p_T .

Flavor hierarchy of jet quenching



- A state-of-art jet quenching framework (NLO-pQCD + LBT + Hydrodynamics)
- At $p_T > 30-40$ GeV, B mesons will also exhibit similar suppression effects to charged hadrons and D mesons, which can be tested by future measurements.

Full jet evolution & energy loss in medium



$$E_{\text{jet}} = E_{\text{in}} + E_{\text{lost}} = E_{\text{in}} + E_{\text{rad,out}} + E_{\text{kick,out}} + (E_{\text{th}} - E_{\text{th,in}})$$

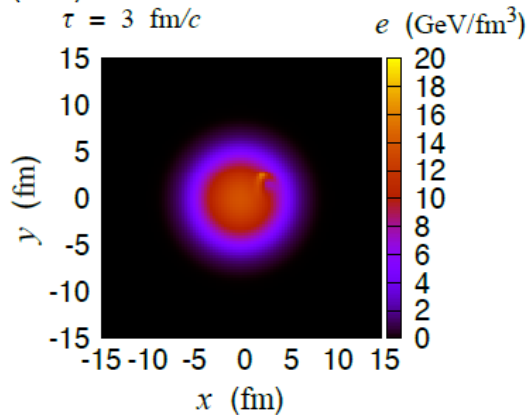
Vitev, Zhang, PRL 2010; GYQ, Muller, PRL, 2011; Casalderrey-Solana, Milhano, Wiedemann, JPG 2011; Young, Schenke, Jeon, Gale, PRC, 2011; Dai, Vitev, Zhang, PRL 2013; Wang, Zhu, PRL 2013; Blaizot, Iancu, Mehtar-Tani, PRL 2013; etc.

Jet evolution & medium response

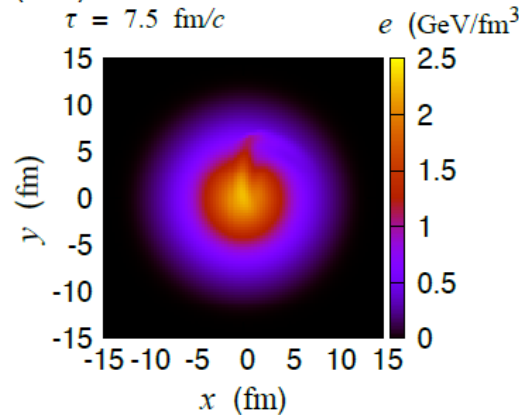
$$\frac{df(\vec{p}, t)}{dt} = C_{coll.E.loss} [f] + C_{coll.broad} [f] + C_{rad} [f]$$

$$\partial_\mu T_{QGP}^{\mu\nu}(x) = J^\nu(x) = -\partial_\mu T_{jet}^{\mu\nu}(x) = -\frac{dP_{jet}^\nu}{dt d^3x} = -\sum_j \int \frac{d^3k_j}{\omega_j} k_j^\nu k_j^\mu \partial_\mu f_j(\mathbf{k}_j, \mathbf{x}, t)$$

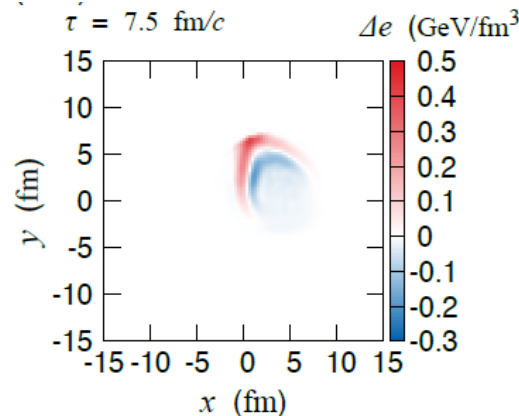
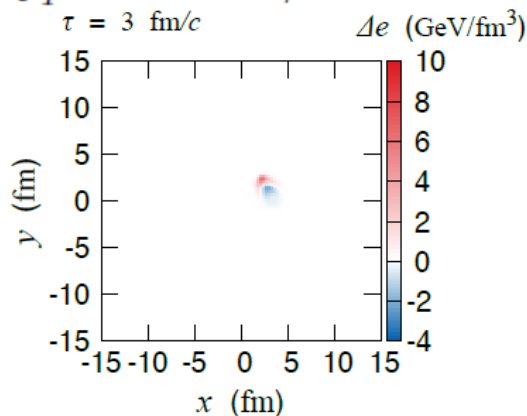
(a-1)



(a-2)



$p_T^{\text{jet}} = 150 \text{ GeV}/c \quad (x_0^{\text{jet}}, y_0^{\text{jet}}) = (0 \text{ fm}, 6.54 \text{ fm}) \quad \phi_p = 5\pi/8$



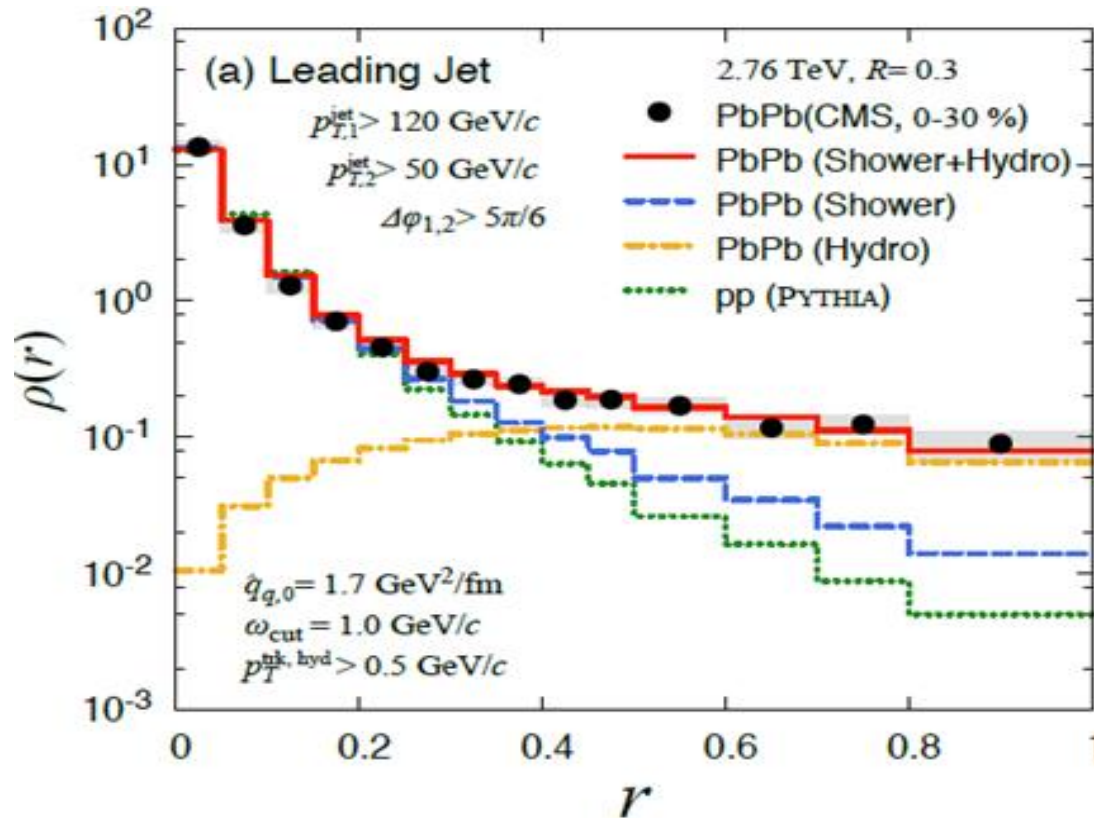
- V-shaped wave fronts are induced by the jet, and develop with time
- The wave fronts carry the energy & momentum, propagates outward & lowers energy density behind the jet
- Jet-induced flow and the radial flow of the medium are pushed and distorted by each other

Chang, GYQ, PRC 2016

Tachibana, Chang, GYQ, PRC 2017

Chang, Tachibana, GYQ, PLB 2020

Effect of jet-induced flow on jet shape



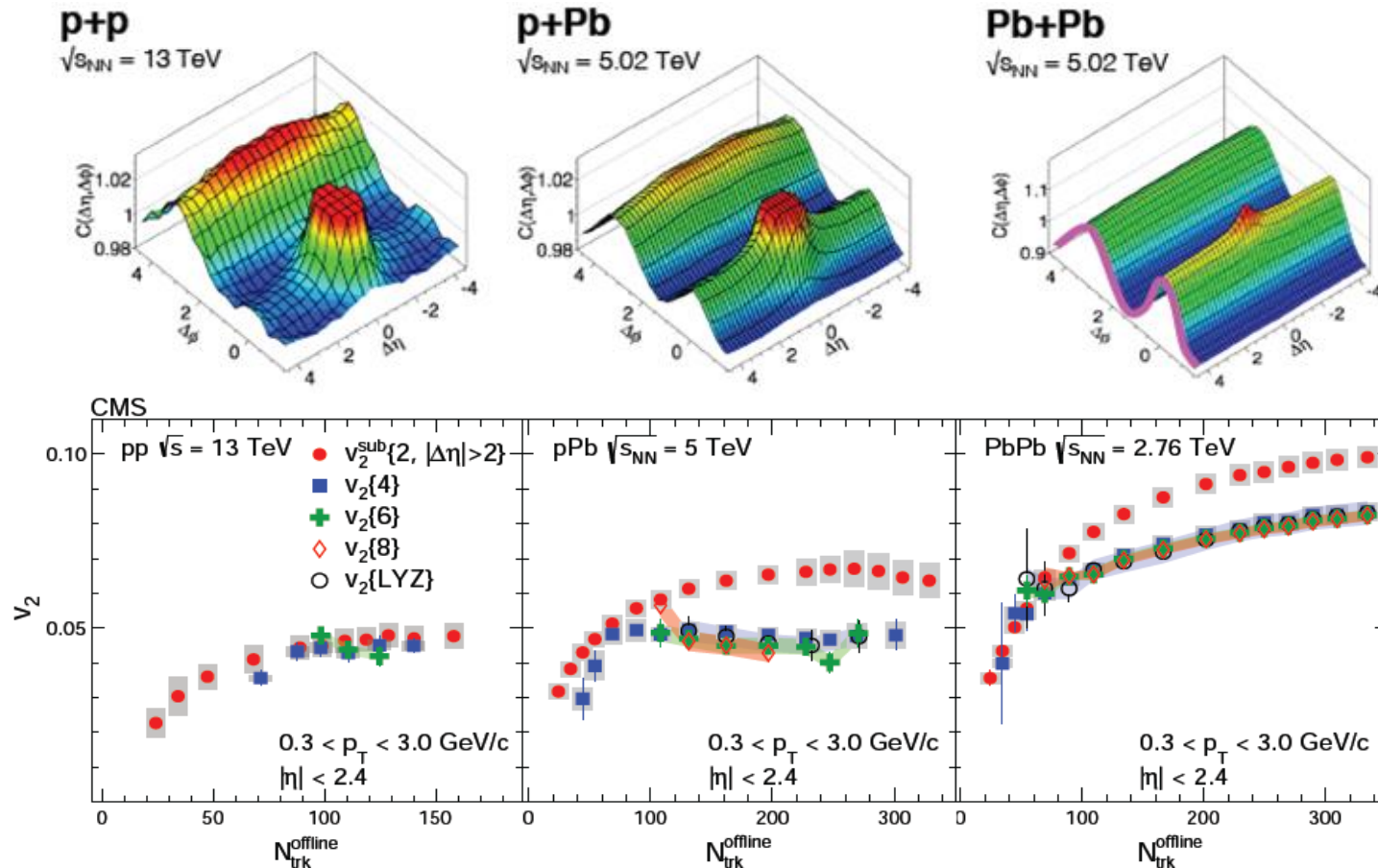
The contribution from the hydro part is quite flat and finally dominates over the shower part in the region from $r = 0.4-0.5$.

Signal of jet-induced medium excitation in full jet shape at large r .

Flow and jets in small systems

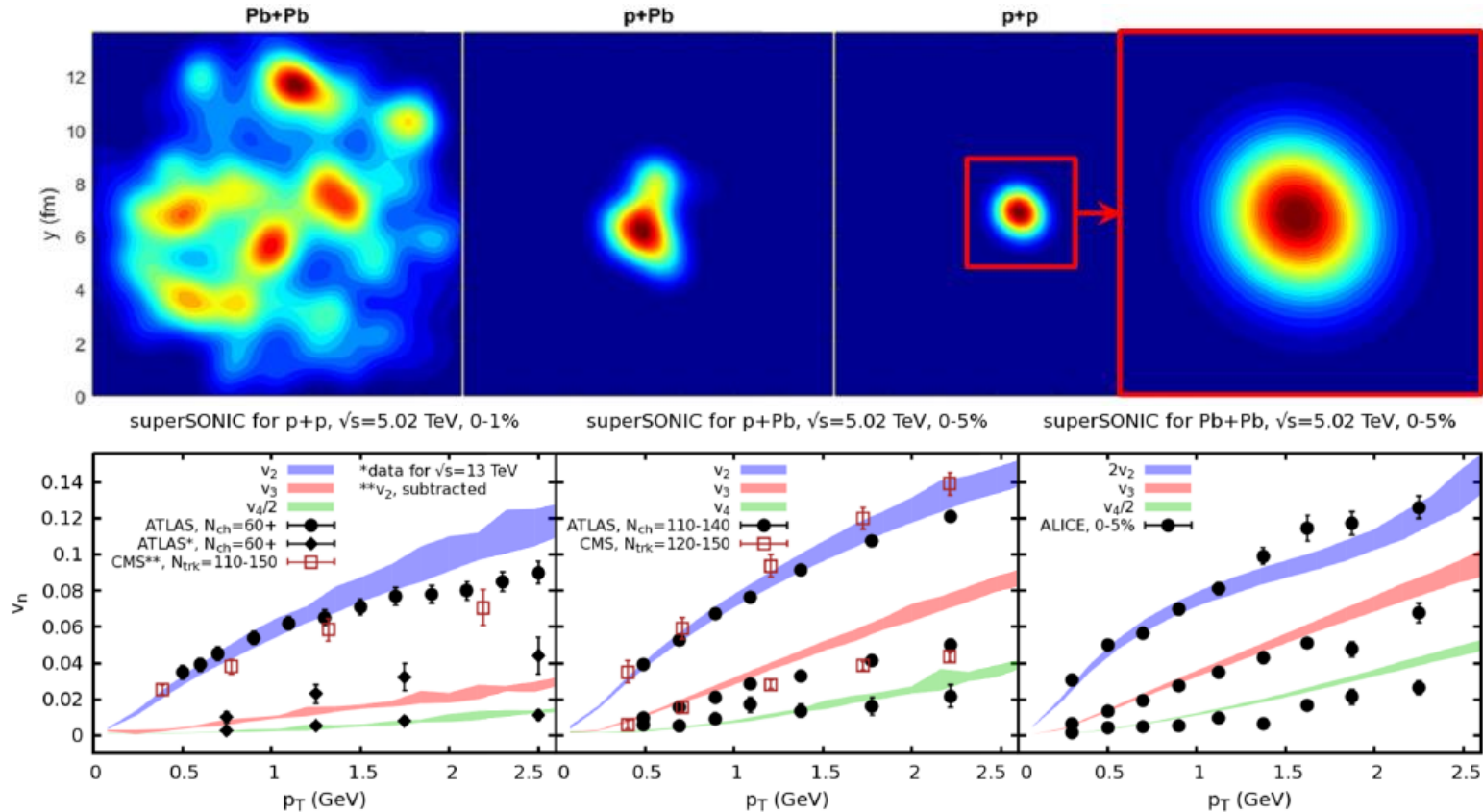
Flow in small collision systems

- Plenty of evidences for strong collectivity in small collision systems



What is the dynamical origin of the observed collectivity?

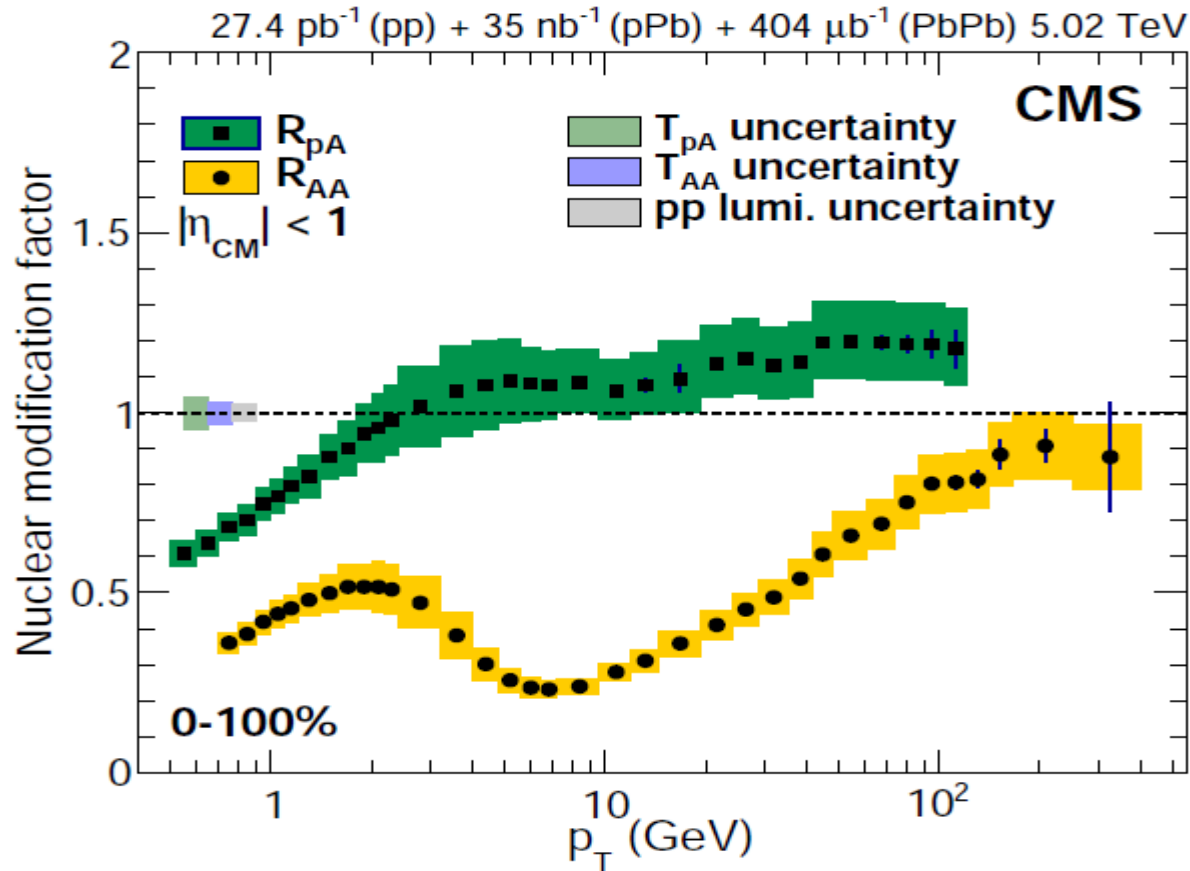
Formation of mini-QGP?



- The flow harmonics can be viewed as the final-state effect due to hydrodynamic evolution of small collisional systems with certain amount of initial anisotropy.

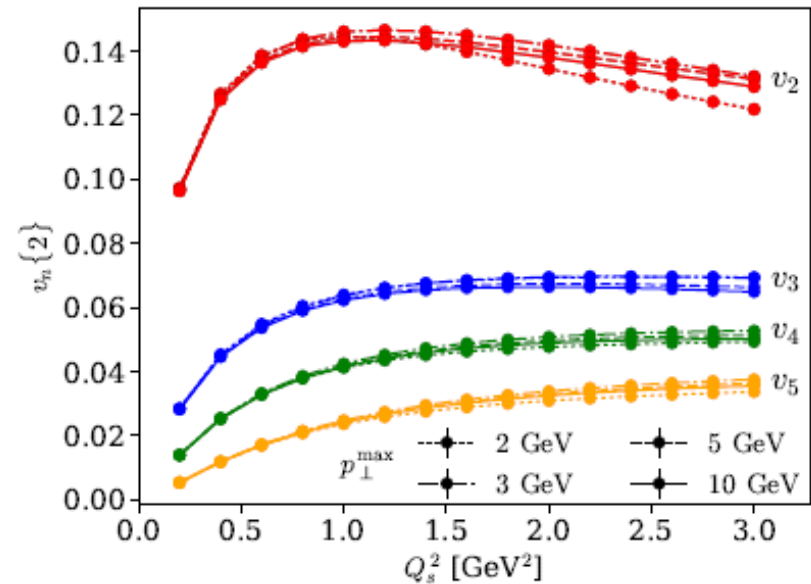
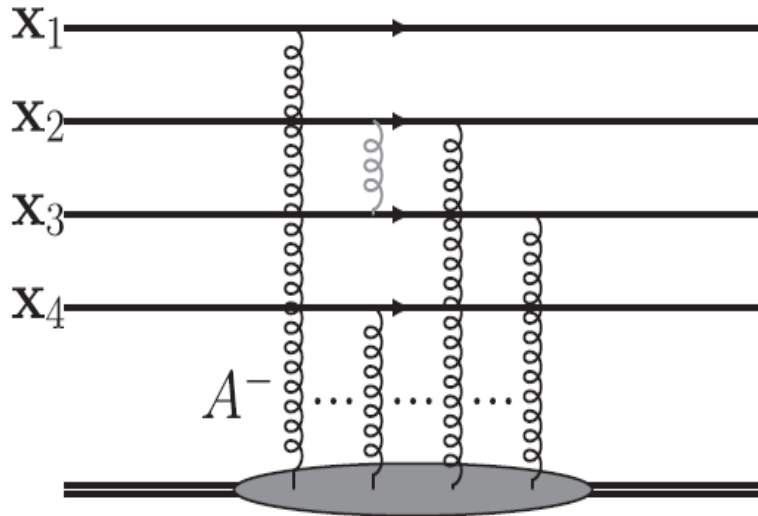
Bozek, Broniowski, Torrieri, PRL 2013; Bzdak, Schenke, Tribedy, Venugopalan, PRC 2013; GYQ, Muller, PRC 2014; Bzdak, Ma, PRL 2014; Weller, Romatschke, PLB 2017; Zhao, Zhou, Xu, Deng, Song, PLB 2018; etc.

Signature in hard probes?



- Up to now, there is no jet quenching observed in pA collisions

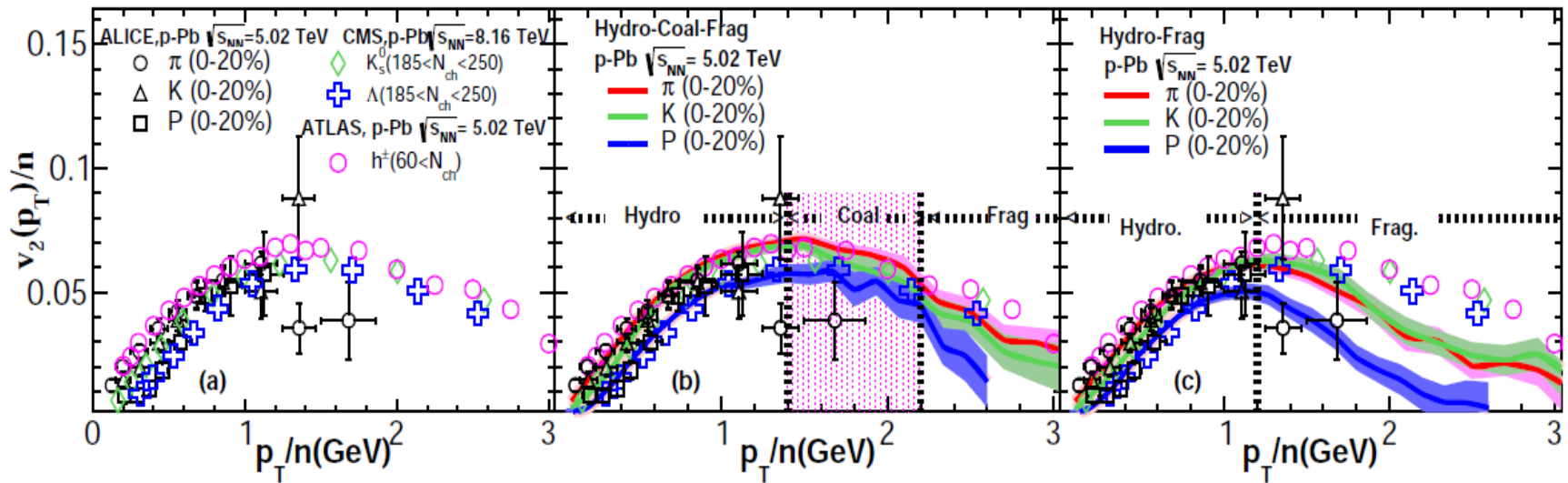
Or initial state effect?



- In color glass condensate (CGC) dilute-dense factorization framework or the saturation formalism, interactions between partons originated from the projectile proton and dense gluons inside the target nucleus can provide significant amount of collectivity (correlations) among partons.

Dusling, Mace, Venugopalan, PRL (2018), 1705.00745; PRD (2018), 1706.06260; etc.

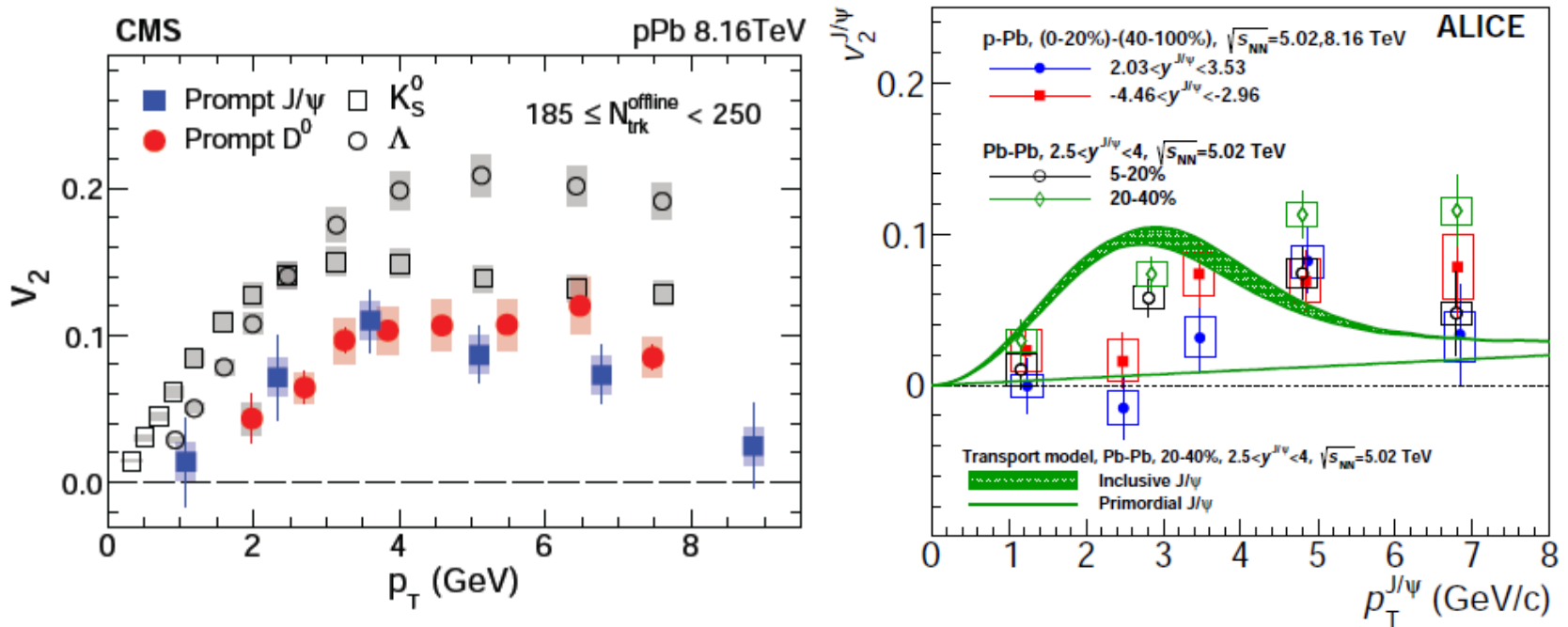
Signature of partonic DOFs in small systems



- To reproduce the observed approximated number of constituent quark (NCQ) scaling of hadron v_2 , it is necessary to include the contribution from the constituent quark coalescence at intermediate p_T (below 6 GeV).
- This result shows the importance of partonic degrees of freedom and supports the formation of mini QGP in high multiplicity p-Pb collisions at the LHC.

Flow of heavy hadrons in small systems

- Charm hadrons also have sizable collectivity in small collision systems.

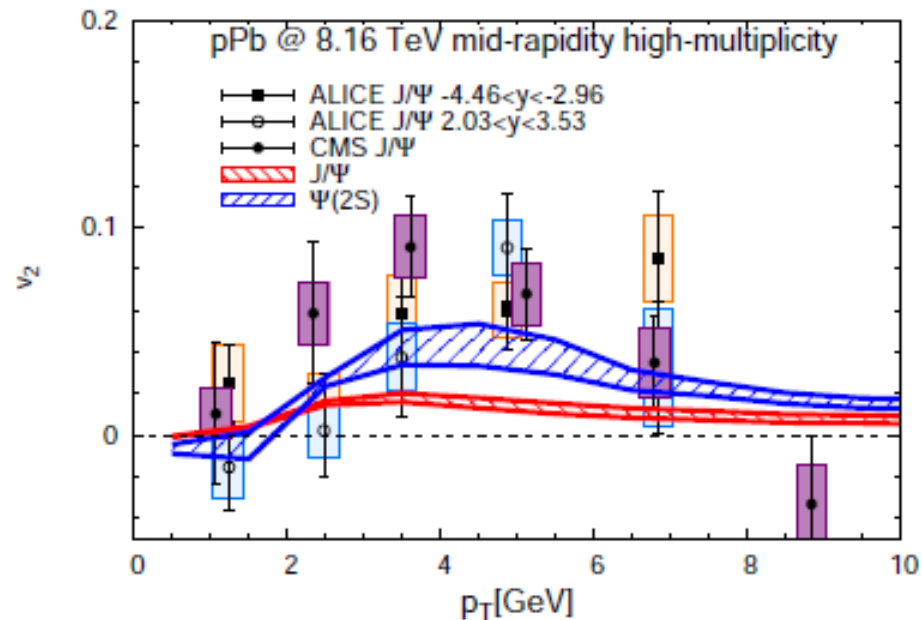


- Large values of elliptic flow v_2 for J/ψ mesons and for D^0 mesons in pPb collisions at the LHC, although they are slightly less than the v_2 values of light hadrons

Initial or final state effect?

J/Ψ v_2 from final state interaction

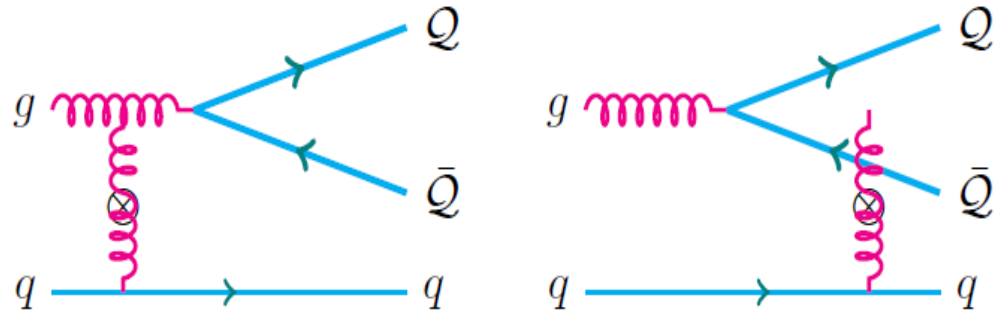
- It is difficult for hydrodynamics to generate large collectivity for heavy mesons, since heavy quark in general does not flow as much as the light quark or gluon due to the large quark mass.



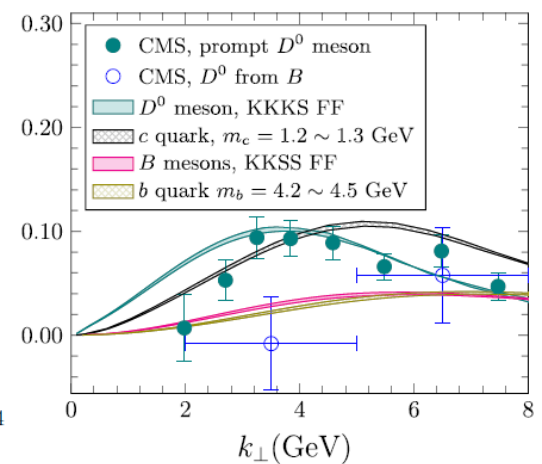
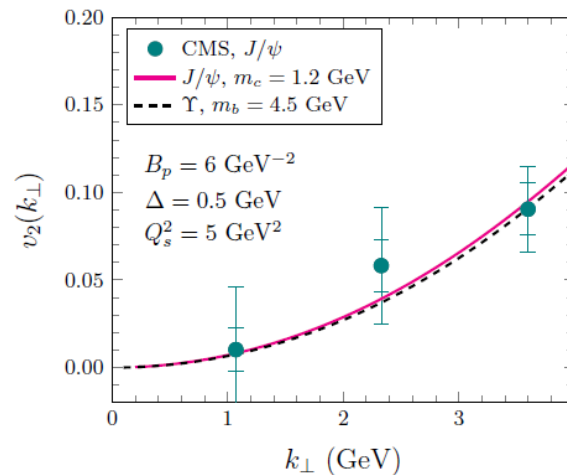
- The final state interactions can only provide a small fraction of the observed v_2 for J/Ψ mesons

J/Ψ v₂ from initial state correlations

- J/Ψ production together with a reference light quark (which fragments into light hadrons)
- Based on the dilute-dense factorization in color glass condensate (CGC) and the color evaporation model (CEM)
- J/Ψ v₂ can be generated from the interaction between partons from the proton projectile and dense gluons in the nuclear target
- v₂ for other heavy mesons



$$v_2[\text{J}/\Psi] = V_{2\Delta}[\text{J}/\Psi, \text{ref}] / v_2[\text{ref}]$$

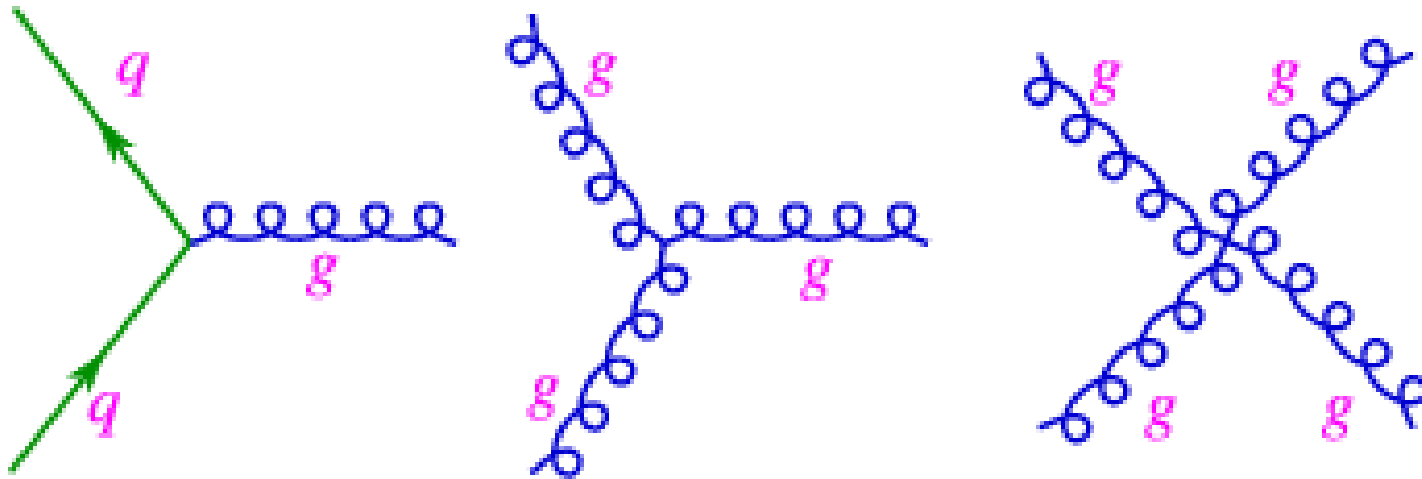


Summary

- **Flow and bulk properties**
 - Explore the transport properties of the QGP at higher precision
 - Spectra, flow, fluctuations, correlations, etc. for different collision energies and system sizes (centralities)
- **Jets and heavy flavors**
 - Characterize the macroscopic properties and microscopic structures of the QCD matter
 - Heavy and light flavor jet and jet structure (substructure) observables
- **Small systems**
 - Understand the dynamical origins of the collectivity and correlations of heavy and light particles observed in pp, pA and AA collisions
 - Search for the smallest QGP

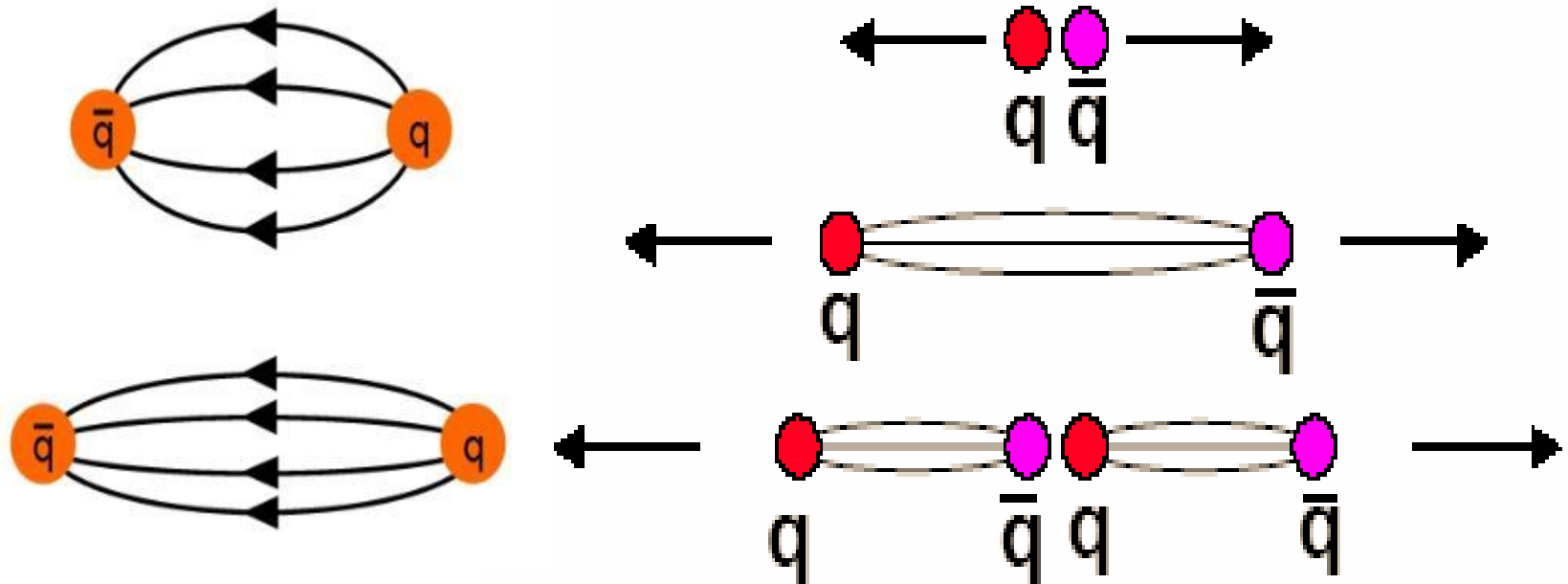
The theory of strong-interaction

- Quantum chromodynamics (QCD): quantum field theory of strong-interaction
- Fundamental fields: quarks and gluons. Both carry “color” charges.



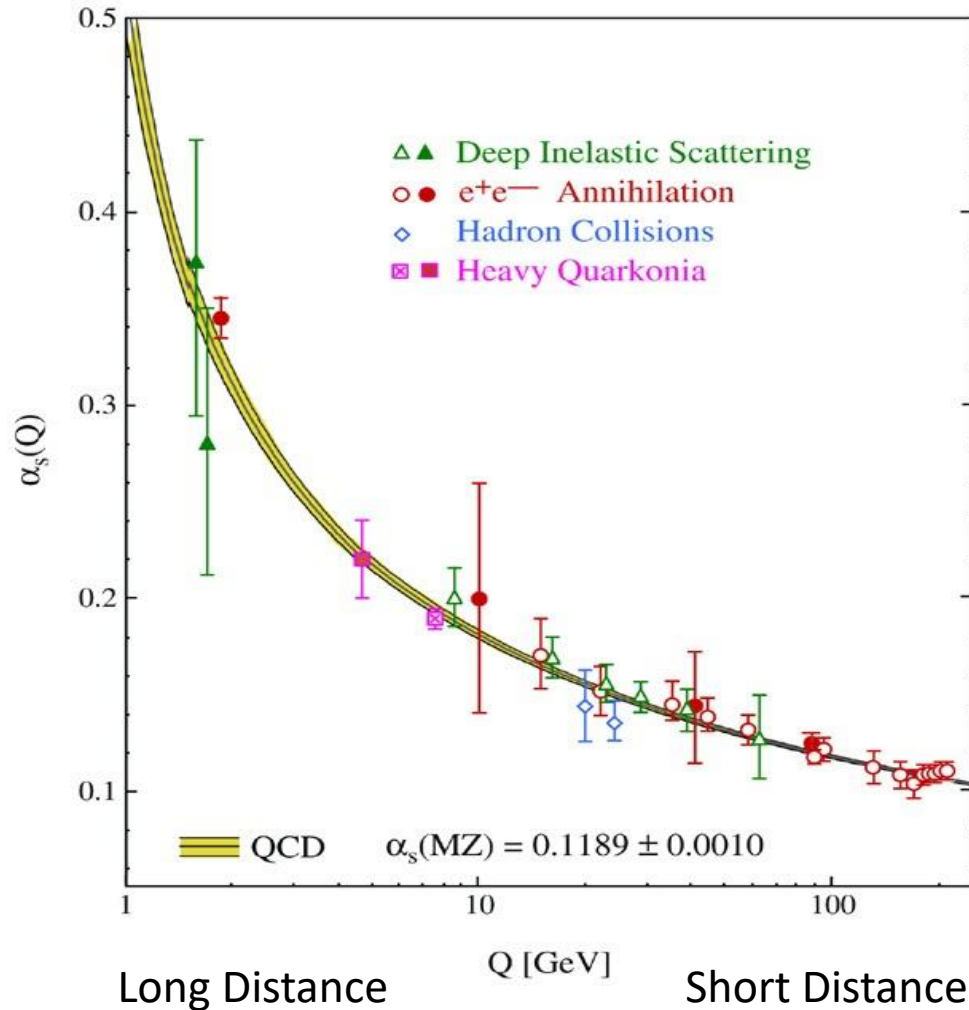
- Two main properties: color confinement and asymptotic freedom

Color confinement of QCD



- Due to the gluon self-interaction, effective color charges increase with distance => Coupling becomes large at large distance.
- Quarks are confined within hadrons. No free quarks have been observed.

Asymptotic freedom of QCD

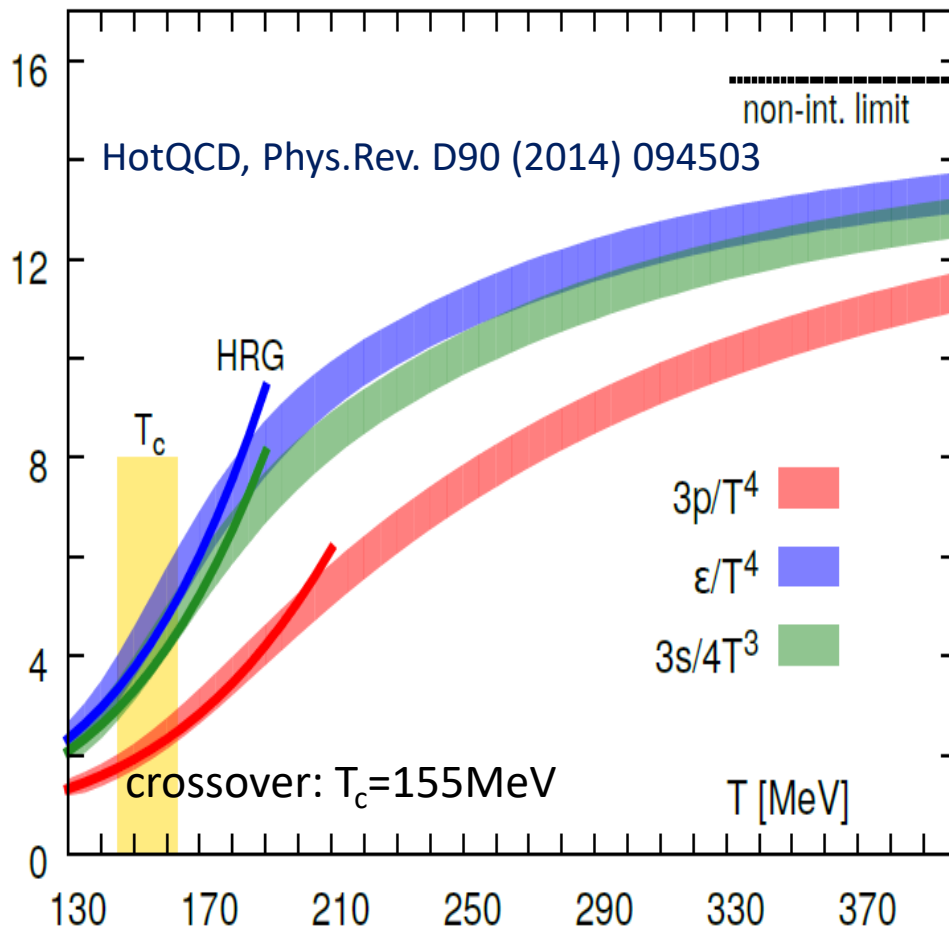


2004 Nobel Prize:
"for the discovery of asymptotic freedom in the theory of the strong interaction".



David Gross , David Politzer, Frank Wilczek

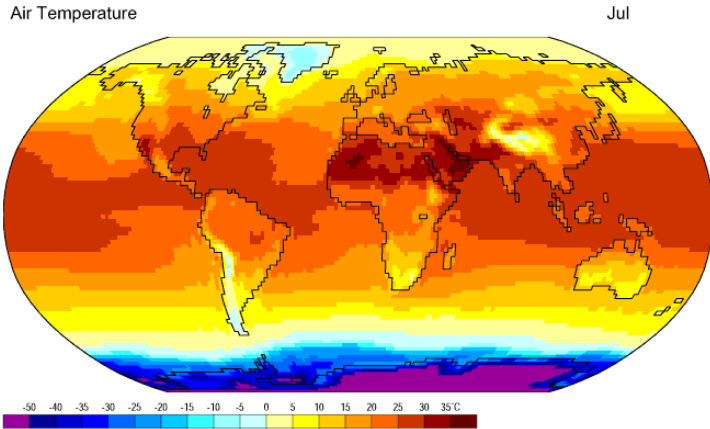
Heating up nuclear matter via lattice QCD



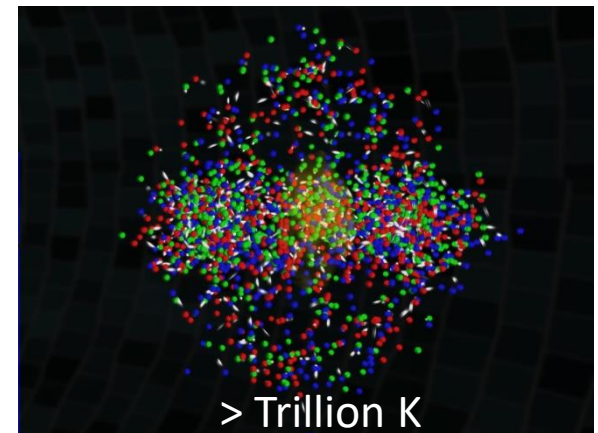
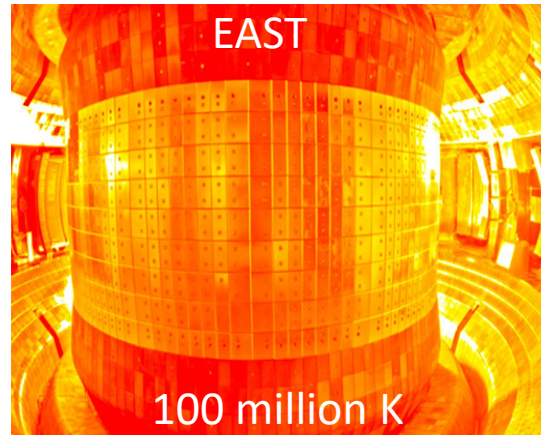
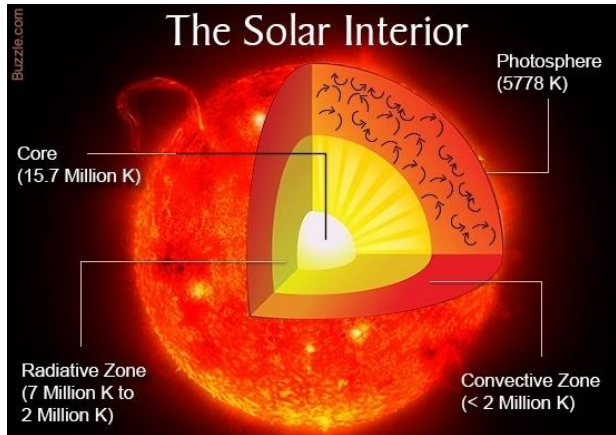
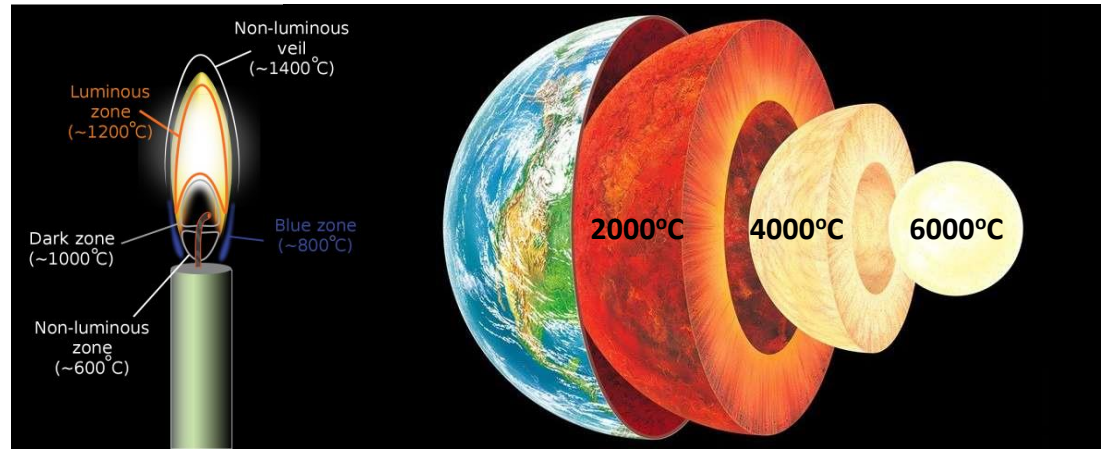
- A transition (crossover) between hadronic matter and quark-gluon matter at $T_c=155\text{MeV}$
- $T < T_c$, the thermodynamics of the system can be described by hadron resonance gas model
- $T=400\text{MeV}$, the partonic system is still strongly-interacting, not close to non-interacting quark-gluon gas
- For non-interacting massless gas: $P = d \frac{\pi^2}{90} T^4$

$$T_c = 155\text{MeV}/k = (155 \cdot 10^6 \text{eV}) \cdot (1.6 \cdot 10^{-19} \text{J/eV}) / (1.38 \cdot 10^{-23} \text{J/K}) = 1.8 \cdot 10^{12} \text{K}$$

How high temperature?

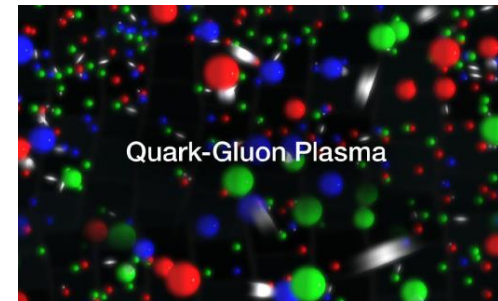
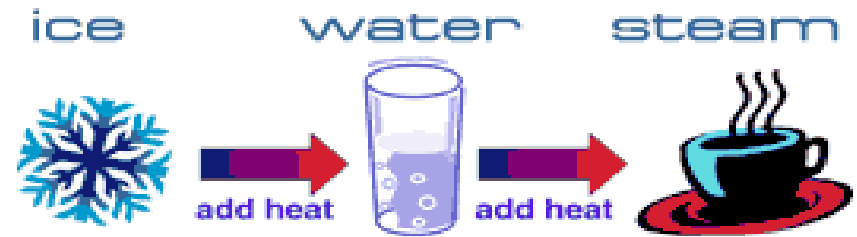


Data: NCEP/NCAR Reanalysis Project, 1959-1997 Climatologies

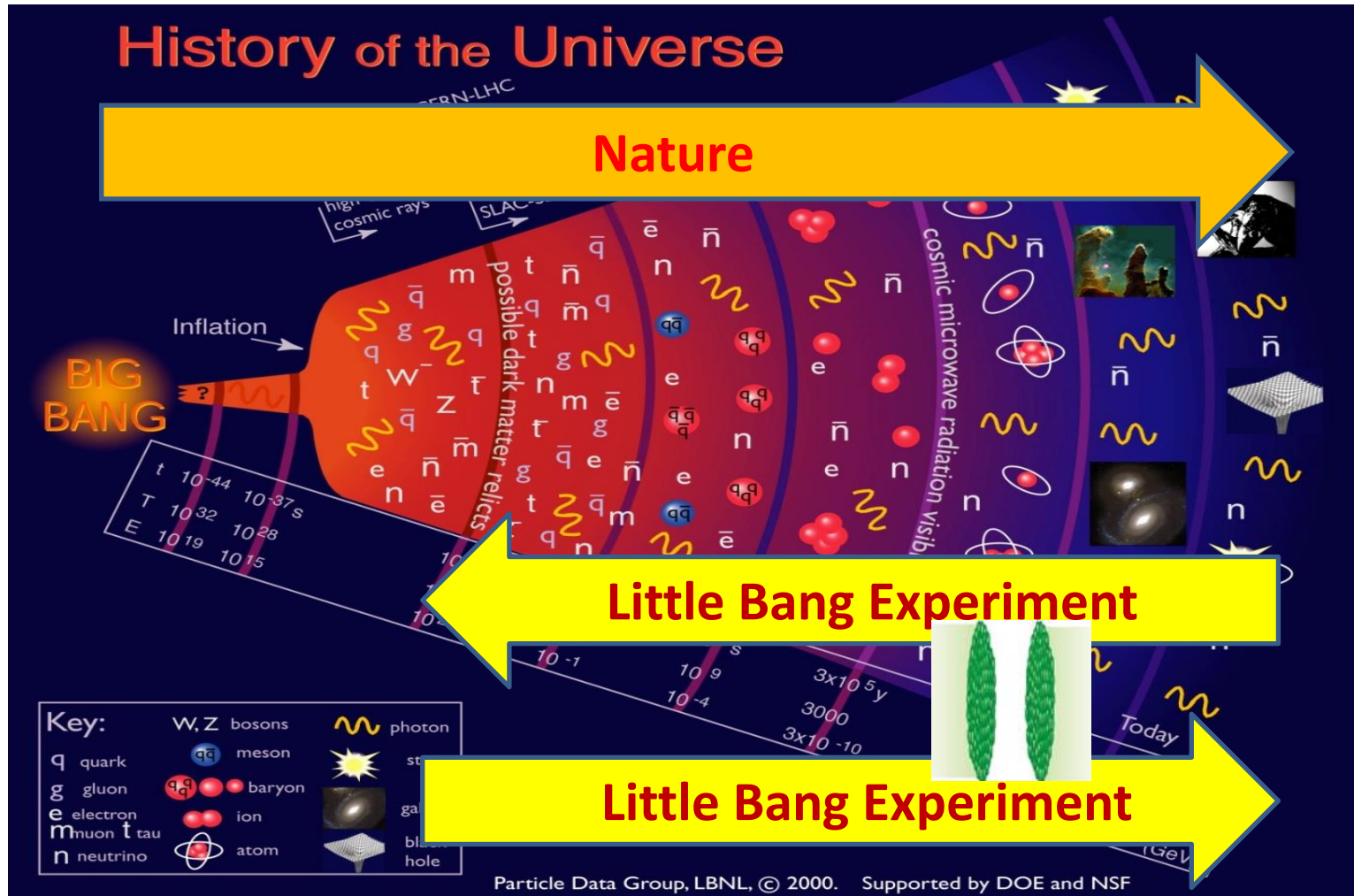


Heating up the matter & states of matter

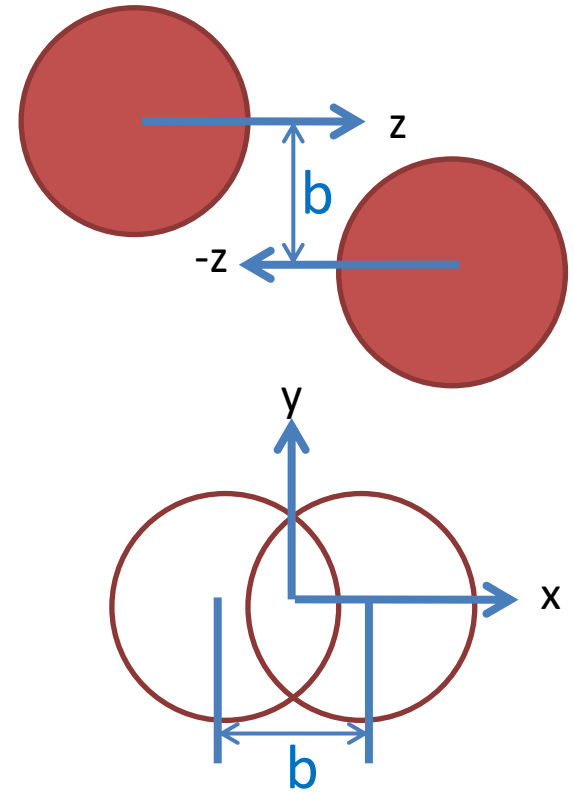
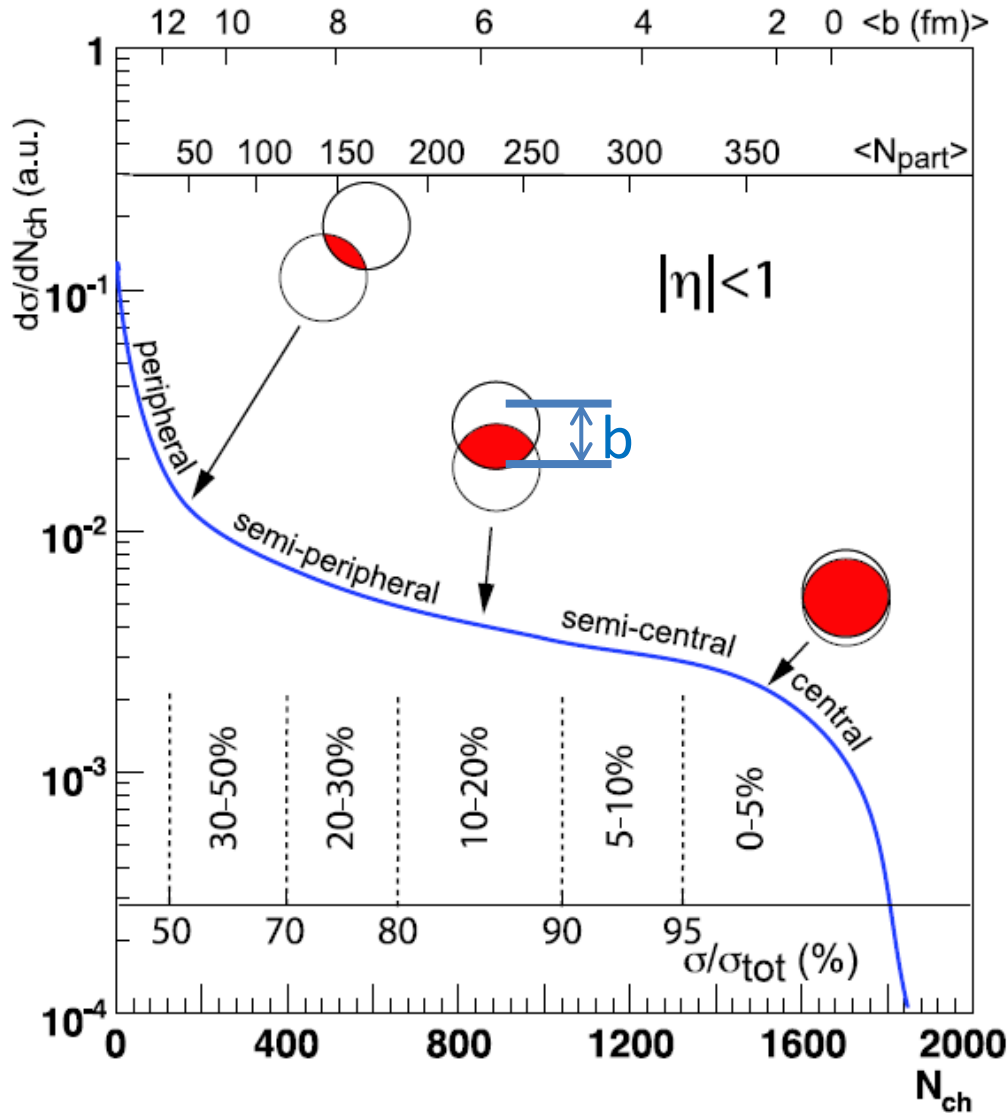
- Increasing temperature increases the kinetic energies of DOFs. High enough temperature may break the larger structures (DOFs) by activating more fundamental DOFs.
- **Molecules (chemical bonds): 10^3K , burning, flame, torch**
- **Atoms (QED plasma): 10^5K , ironization**
- **Nuclei: 10^8K , nuclear reaction**
- **Nucleons (QGP): 10^{12}K , relativistic nuclear collisions (little bangs)**



QGP and early Universe

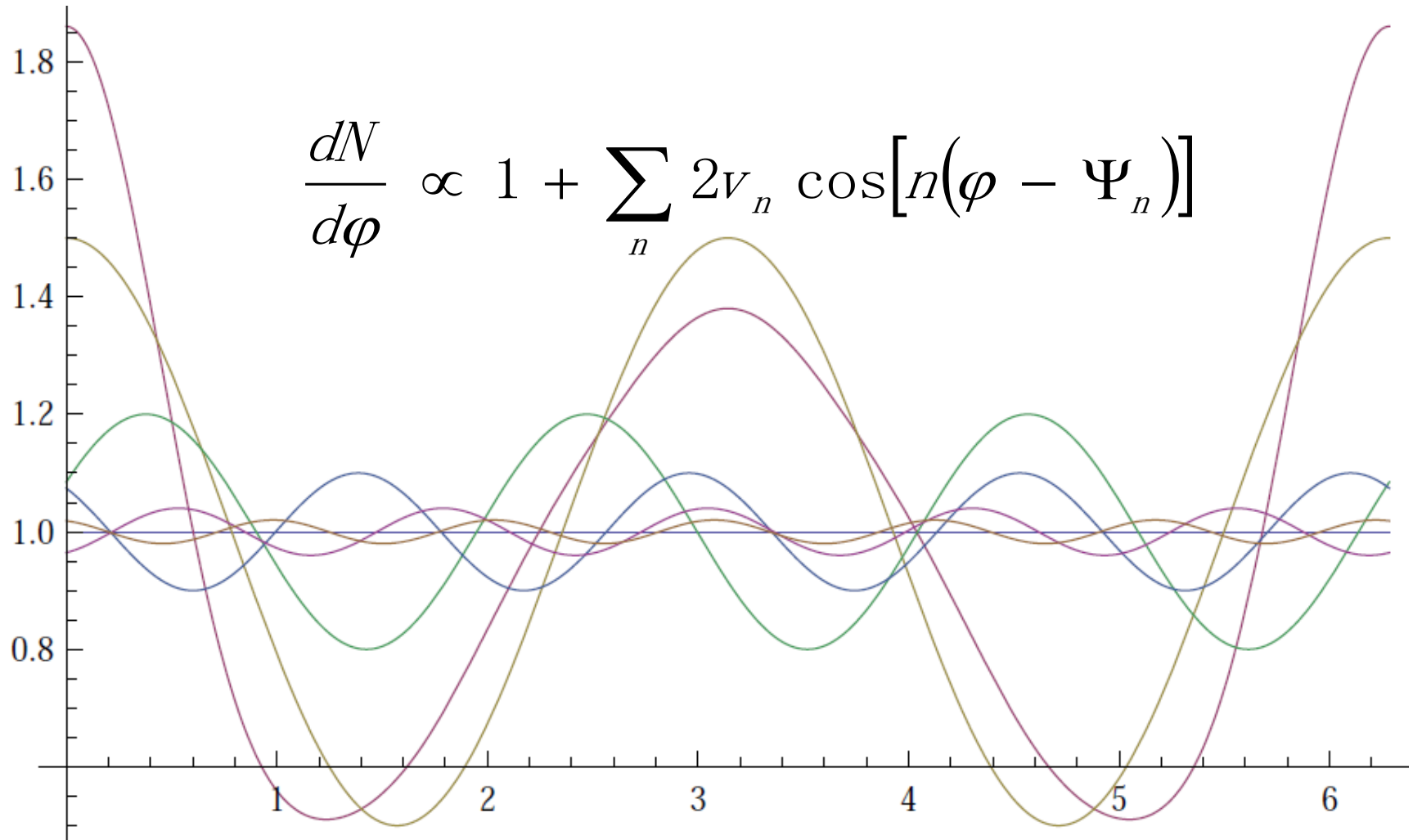


Collision centrality



Miller, Reygers, Sanders,
 Steinberg, *Ann. Rev. Nucl.
 Part. Sci.* 57 (2007) 205-243

Anisotropy: Fourier decomposition



Shear viscosity

- In $\Delta t = \lambda/\bar{v}$, there are on average $\frac{1}{6}n\lambda A_y$ particles from both $y + \lambda$ and $y - \lambda$ passing through the plane at y from above and below.

- The net momentum passing through the plane:

$$\Delta p_x = \frac{1}{6}n\lambda A_y m [u_x(y + \lambda) - u_x(y - \lambda)] = \frac{1}{3}n\lambda^2 A_y m \frac{du_x}{dy}$$

- The drag force:

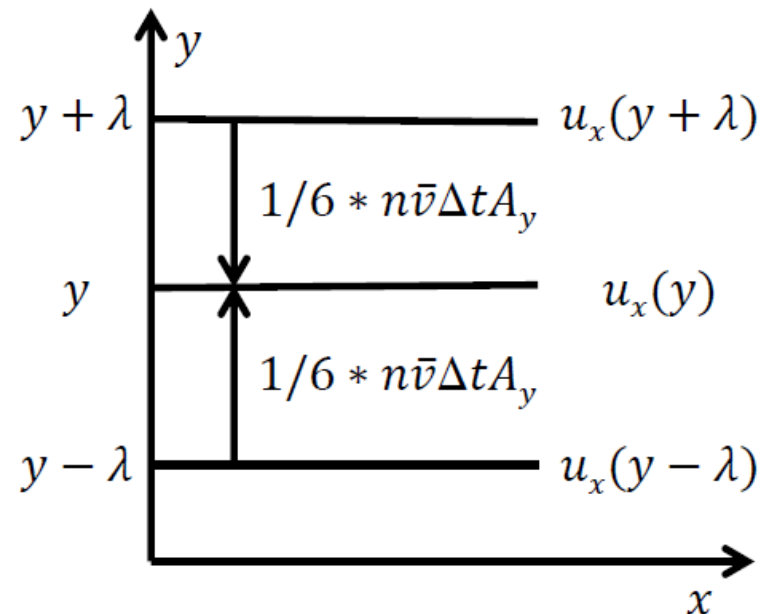
$$F_x = \frac{\Delta p_x}{\Delta t} = \frac{1}{3}n\lambda A_y m \bar{v} \frac{du_x}{dy}$$

- The shear tensor:

$$\frac{F_x}{A_y} = \frac{1}{3}n\lambda m \bar{v} \frac{du_x}{dy} = \eta \frac{du_x}{dy}$$

- The shear viscosity:

$$\eta = \frac{1}{3}n\lambda m \bar{v} = \frac{1}{3}n\lambda \bar{p}$$



Relativistic hydrodynamics

- Energy-momentum conservation:

$$\partial_\mu T^{\mu\nu} = 0$$

$$T^{\mu\nu} = \varepsilon U^\mu U^\nu - (P + \Pi)\Delta^{\mu\nu} + \pi^{\mu\nu}$$

- Equations of motion (Israel-Stewart viscous hydrodynamics):

$$\dot{\varepsilon} = -(\varepsilon + P + \Pi)\theta + \pi^{\mu\nu}\sigma_{\mu\nu}$$

$$(\varepsilon + P + \Pi)\dot{U}^\alpha = \nabla^\alpha(P + \Pi) + \dot{U}_\mu\pi^{\mu\nu} - \Delta_\nu^\alpha\nabla_\mu\pi^{\mu\nu}$$

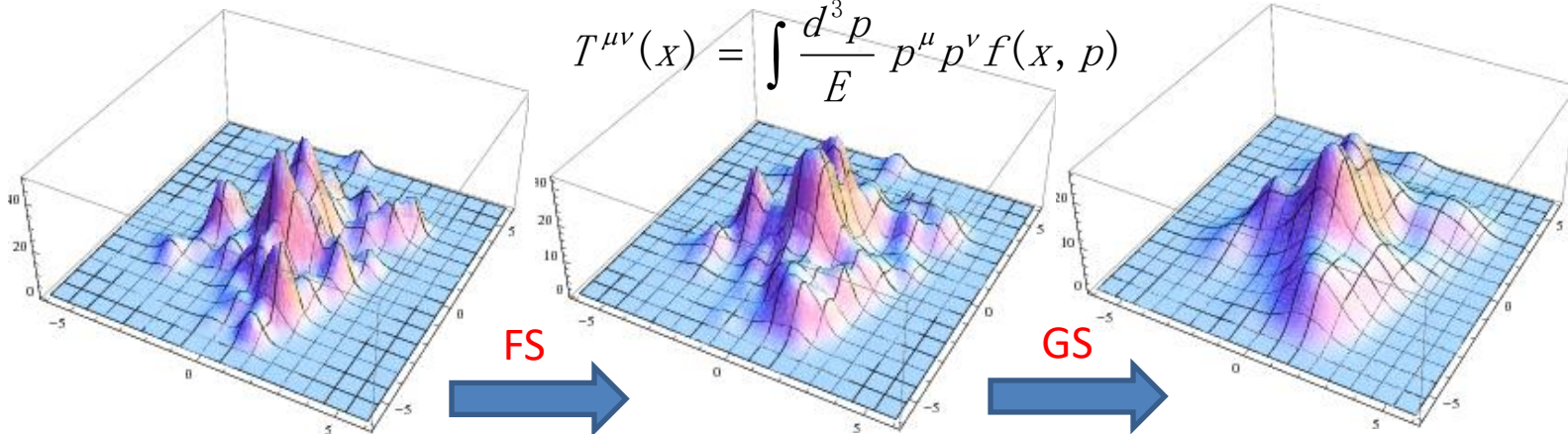
$$\dot{\Pi} = -\frac{1}{\tau_\Pi}\left[\Pi + \zeta\theta + \Pi\zeta T\partial_\alpha\left(\frac{\tau_\Pi}{2\zeta T}U^\alpha\right)\right]$$

$$\Delta_{\alpha\beta}^{\mu\nu}\dot{\pi}^{\alpha\beta} = -\frac{1}{\tau_\pi}\left[\pi^{\mu\nu} - 2\eta\sigma^{\mu\nu} + \pi^{\mu\nu}\eta T\partial_\alpha\left(\frac{\tau_\pi}{2\eta T}U^\alpha\right)\right]$$

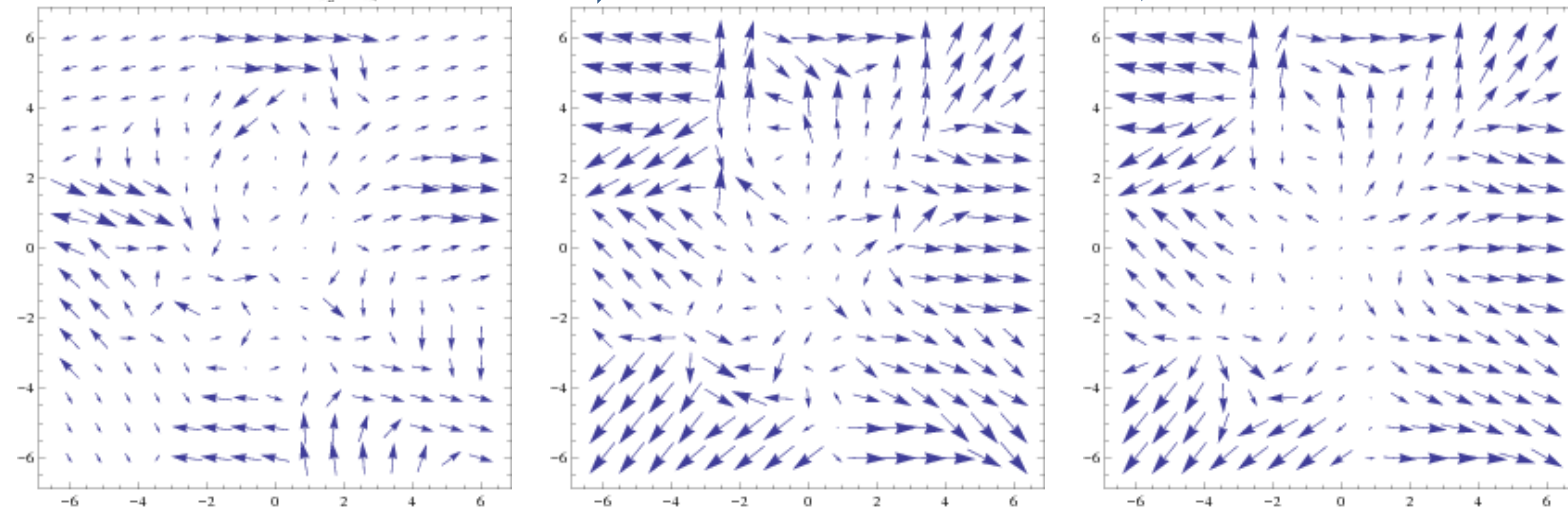
- Equation of state: $P = P(\varepsilon)$

Initial conditions before hydro

$$T^{\mu\nu}(x) = \int \frac{d^3 p}{E} p^\mu p^\nu f(x, p)$$



T^{00}



(T^{0x}, T^{0y})

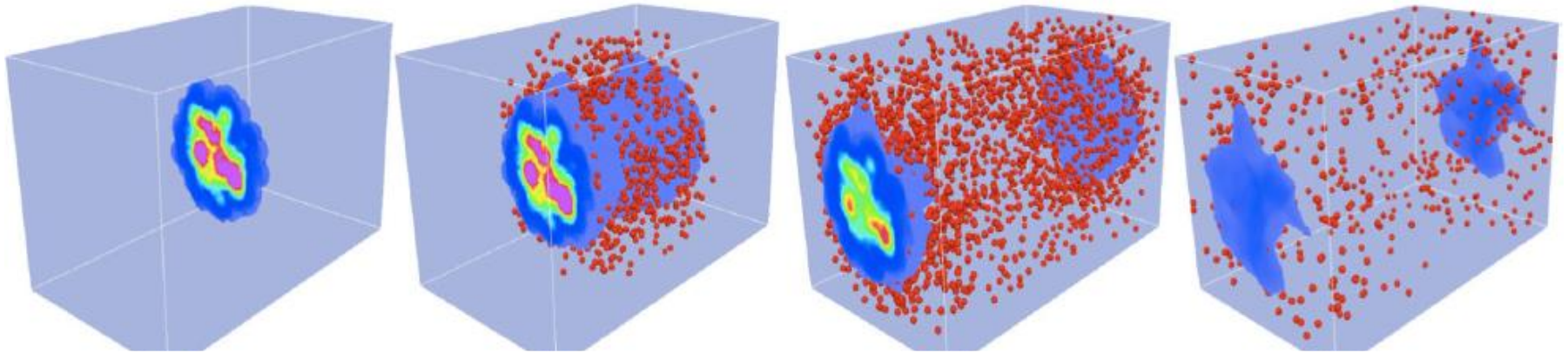
$t_0=0, \sigma_{xy}=0.3\text{fm}$

$t_0=0.6\text{fm}/c, \sigma_{xy}=0.3\text{fm}$

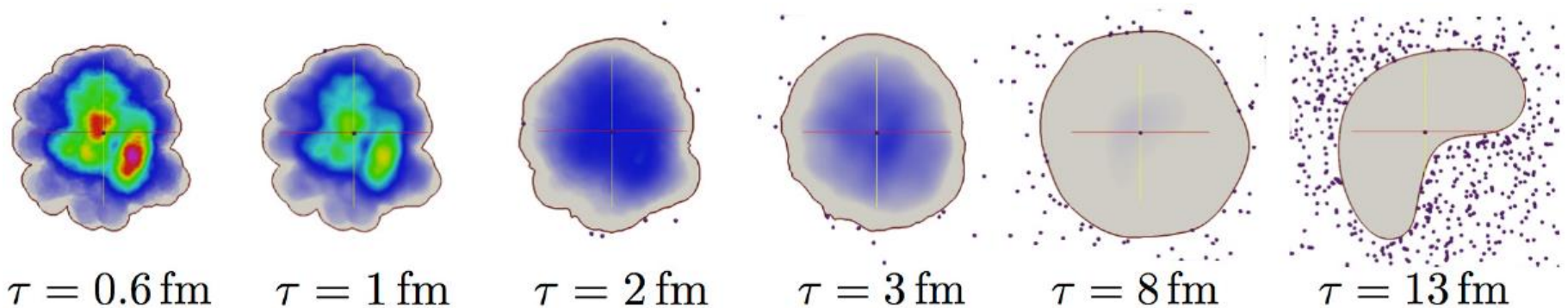
$t_0=0.6\text{fm}/c, \sigma_{xy}=0.5\text{fm}$

$b=8\text{fm}$

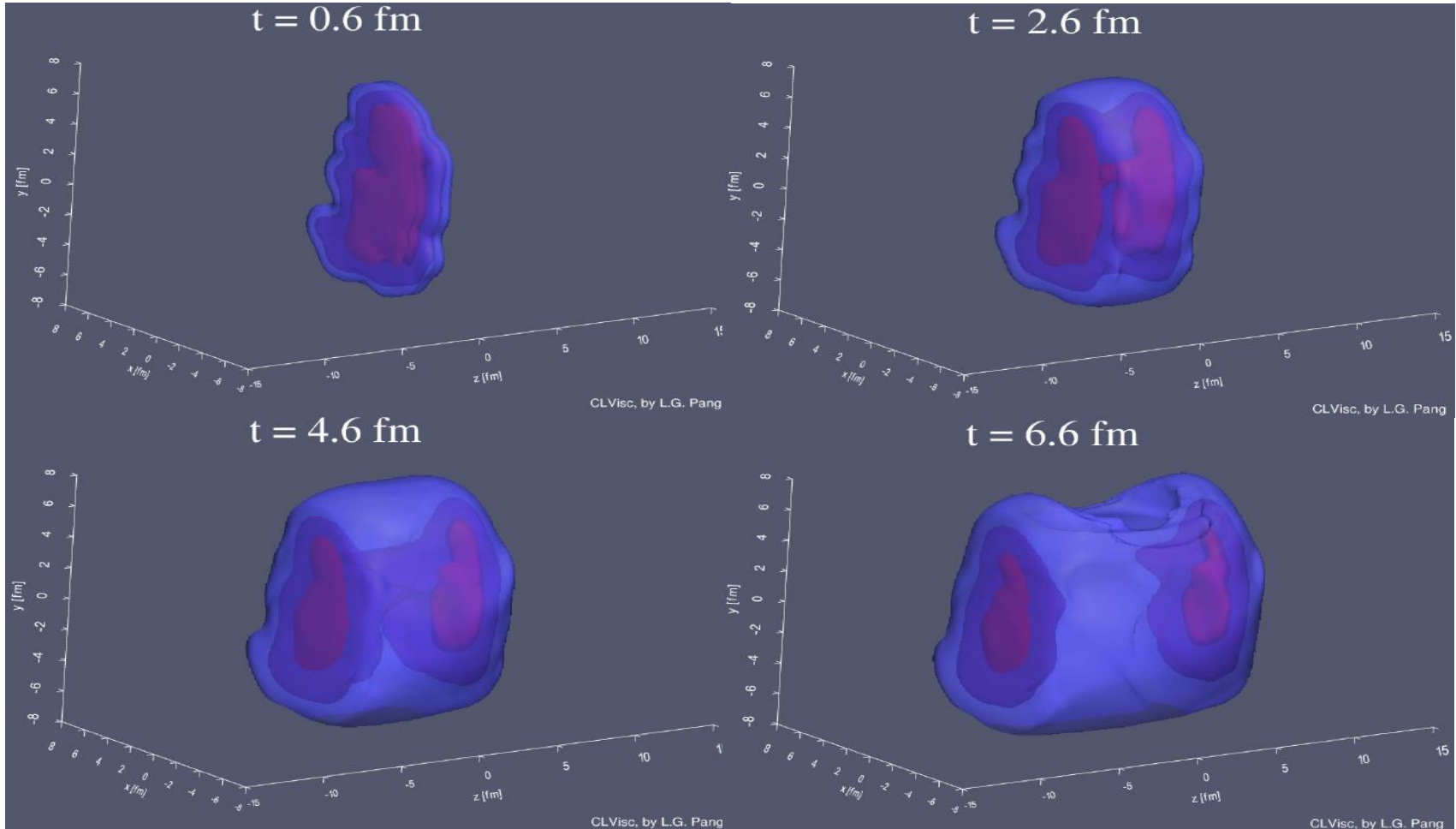
Hydrodynamic evolution of QGP



The color patches are the QGP, and the balls are the final hadrons emitted from the QGP
(from Z. Qiu's Ph.D. thesis, [arXiv:1308.2182](https://arxiv.org/abs/1308.2182))



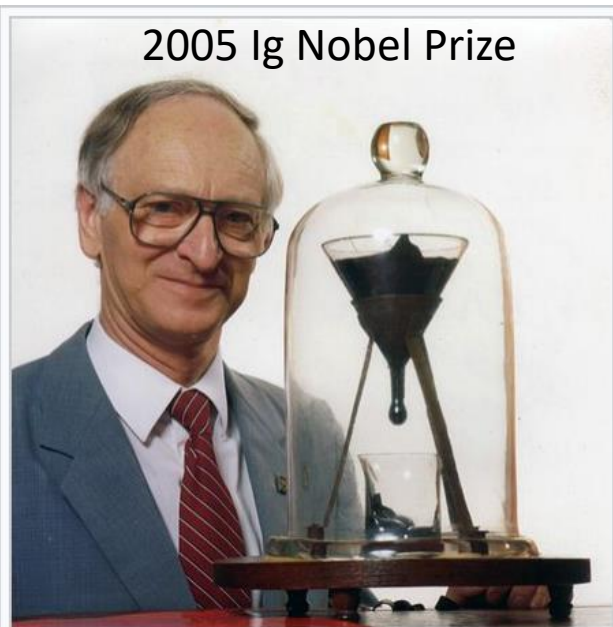
Hydrodynamic evolution of QGP



CCNU-LBNL viscous hydrodynamics (CLVisc) simulation, courtesy of L. G. Pang

沥青滴漏实验

时间	事件	时长 (年)
1927	实验开始	
1930.10	切开封口	
1938.12	第1滴	8.1
1947.2	第2滴	8.2
1954.4	第3滴	7.2
1962.5	第4滴	8.1
1970.8	第5滴	8.3
1979.4	第6滴	8.7
1988.7	第7滴	9.2
2000.11	第8滴	12.3
2014.4	第9滴	13.4



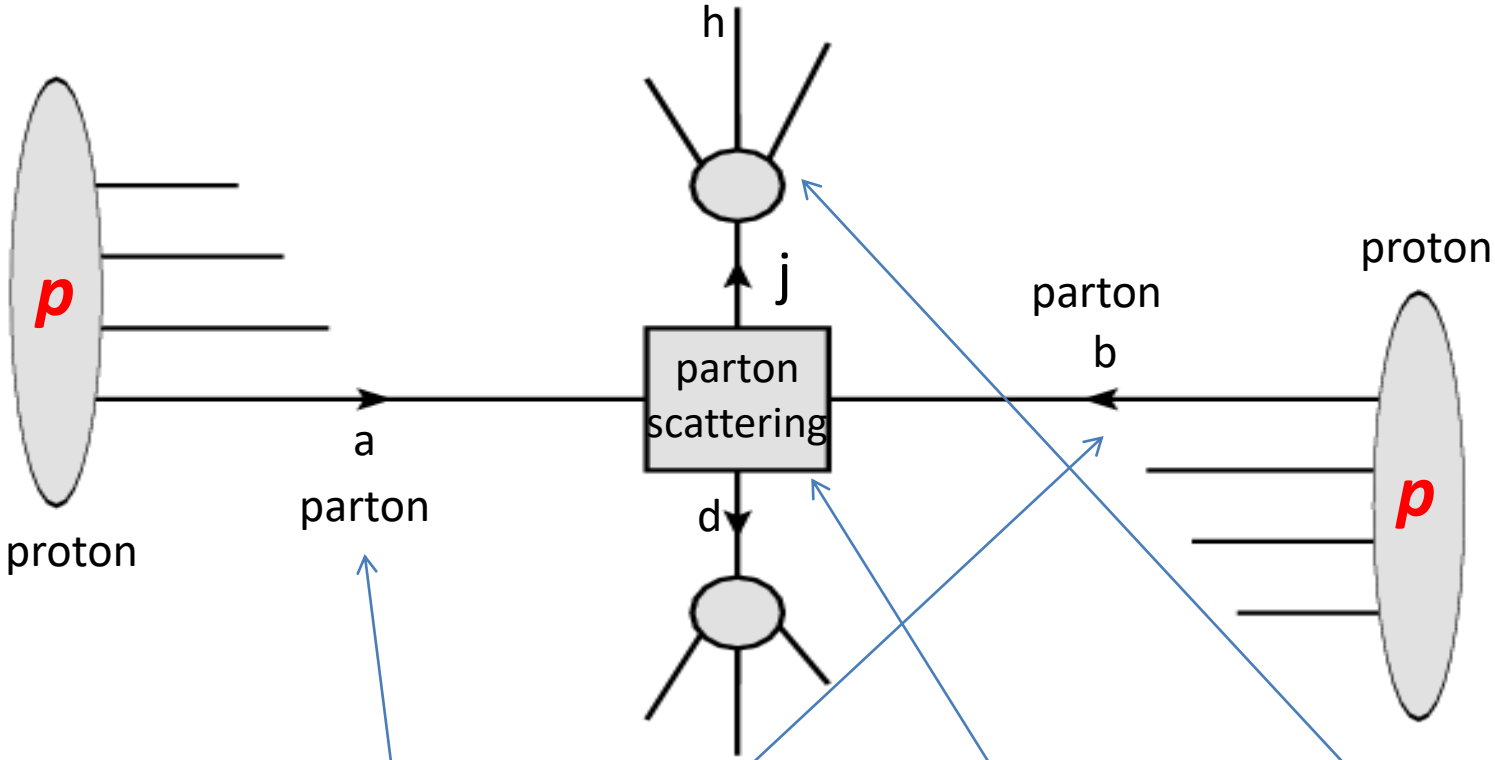
The University of Queensland pitch drop experiment, featuring its then-current custodian, Professor John Mainstone (taken in 1990, two years after the seventh drop and 10 years before the eighth drop fell).

Guinness World Record

for the longest-running laboratory experiment

Edgeworth, Dalton, Parnell, Eur. J. Phys. (1984) 198.

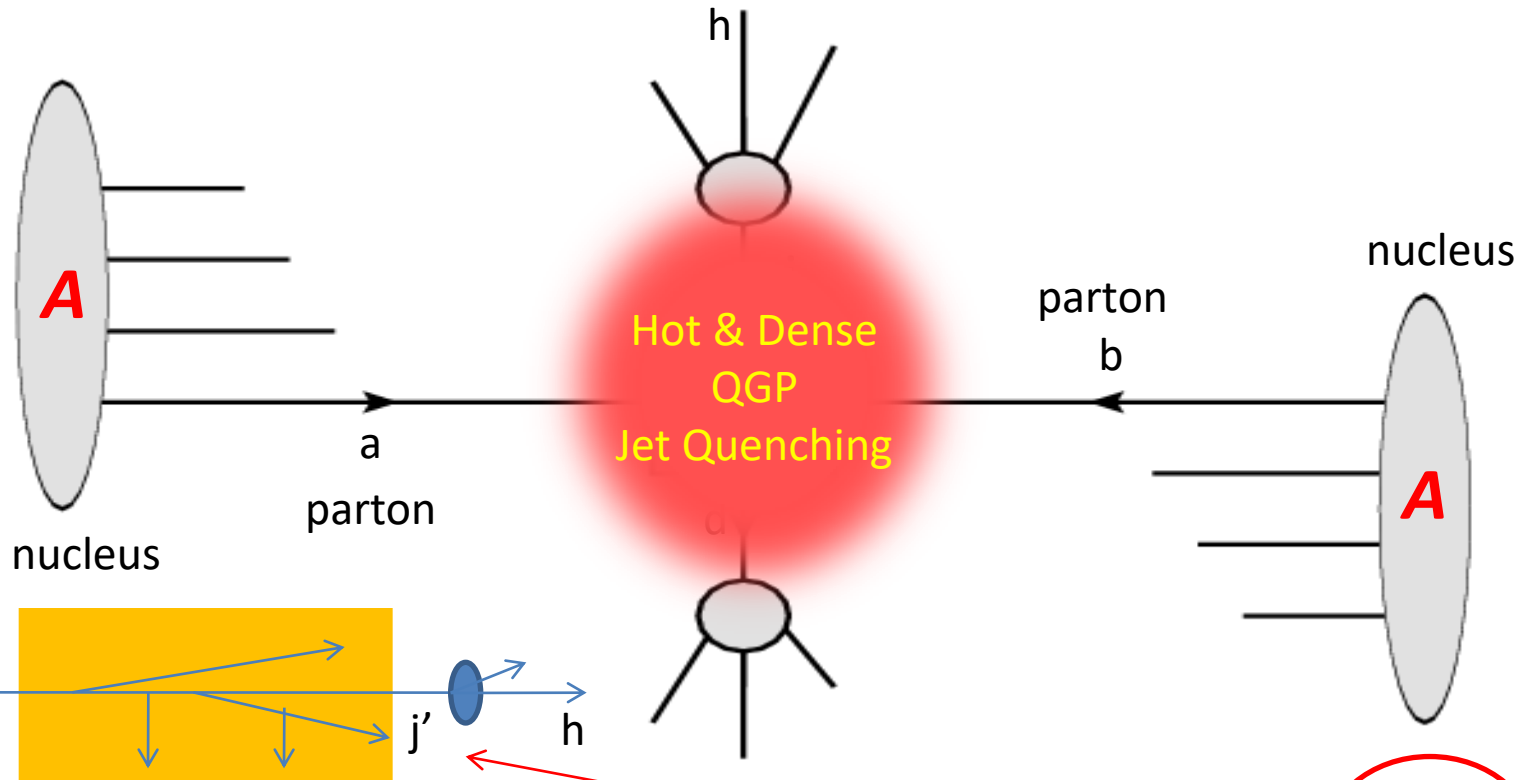
Leading hadron production in pp collisions



$$d\sigma_h = \sum_{abj} f_{a/A} \otimes f_{b/B} \otimes d\sigma_{ab \rightarrow jX} \otimes D_{h/j}$$

pQCD factorization: Large- p_T processes may be factorized into long-distance pieces in terms of PDF & FF, and short-distance parts describing hard interactions of partons.

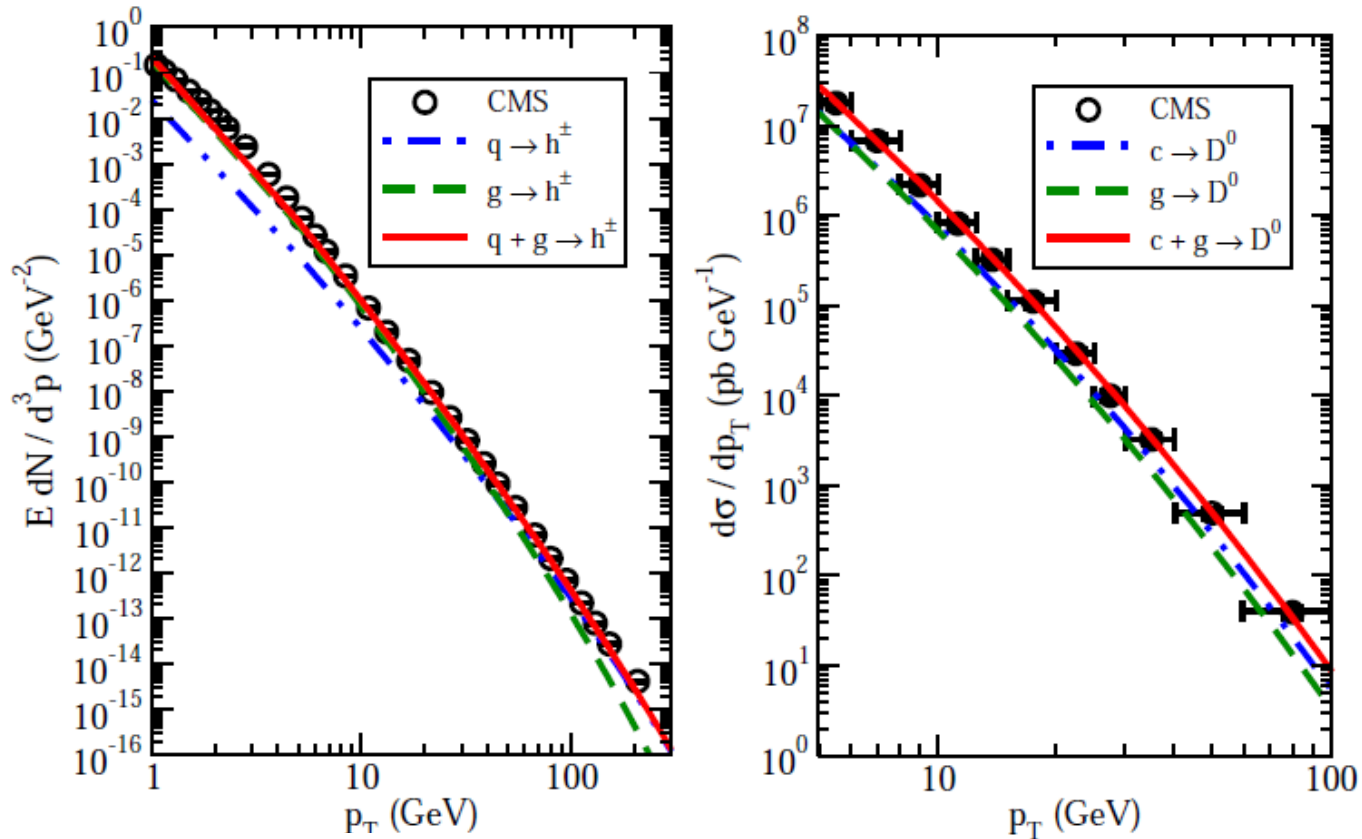
Leading hadron production in AA collisions



$$d\tilde{\sigma}_h = \sum_{abjX} f_{a/A} \otimes f_{b/B} \otimes d\sigma_{ab \rightarrow jX} \otimes \tilde{D}_{h/j}$$

$$d\tilde{\sigma}_h = \sum_{abjj'} f_a \otimes f_b \otimes d\sigma_{ab \rightarrow jX} \otimes P_{j \rightarrow j'} \otimes D_{h/j'}$$

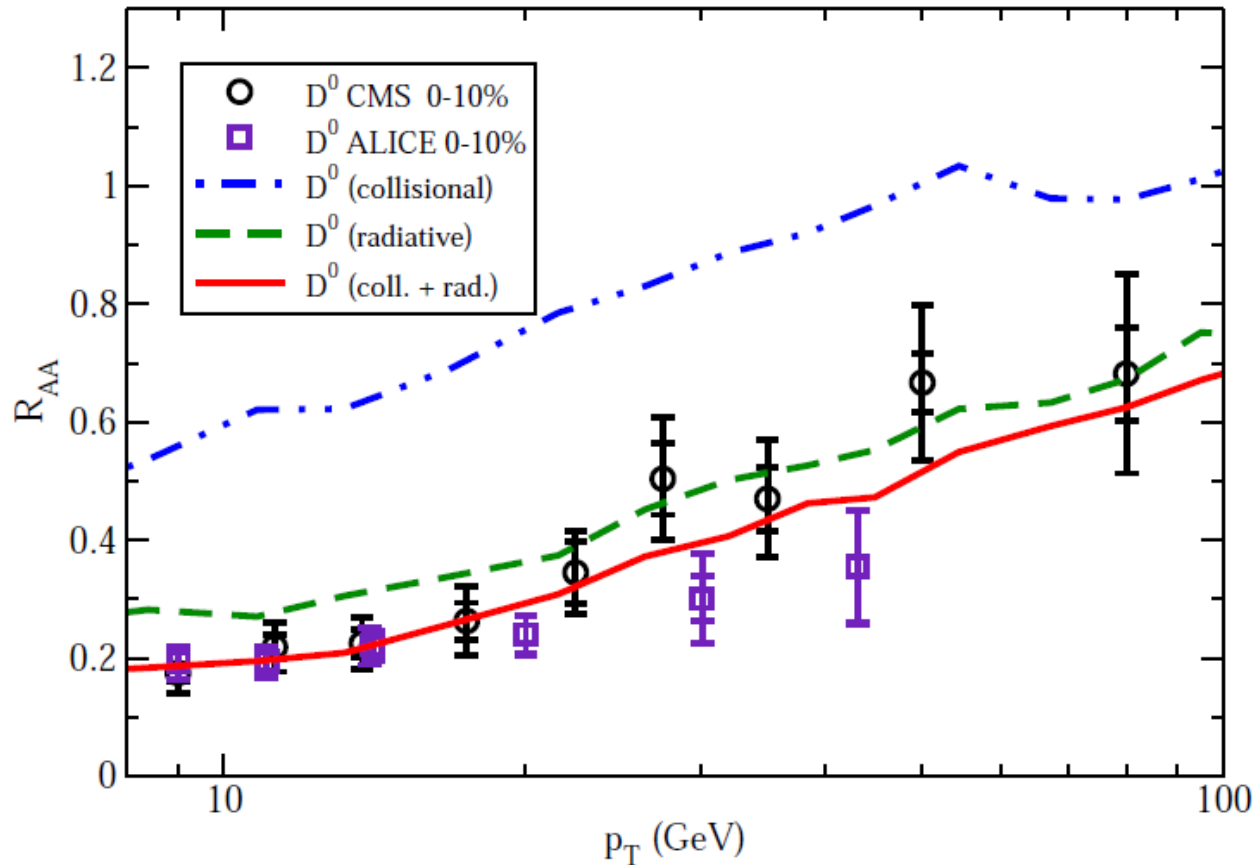
Hadron productions in pp collisions



$$d\sigma_{pp \rightarrow hX} = \sum_{abc} \int dx_a \int dx_b \int dz_c f_a(x_a) f_b(x_b) d\hat{\sigma}_{ab \rightarrow c} D_{h/c}(z_c)$$

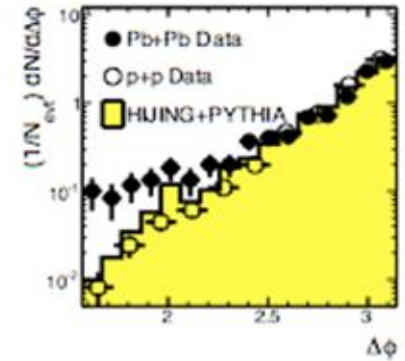
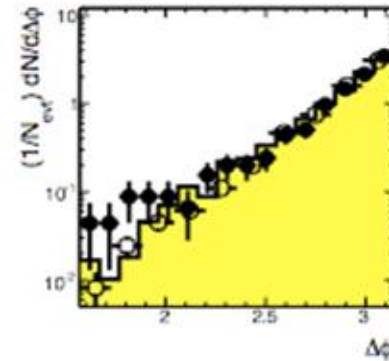
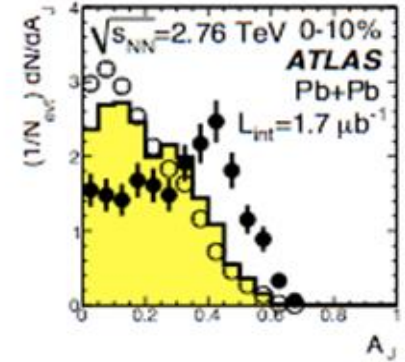
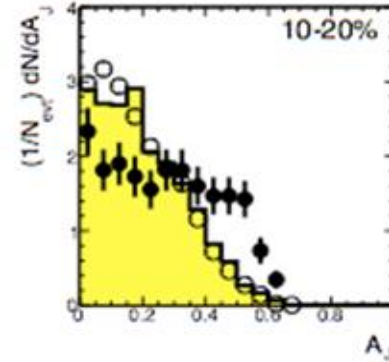
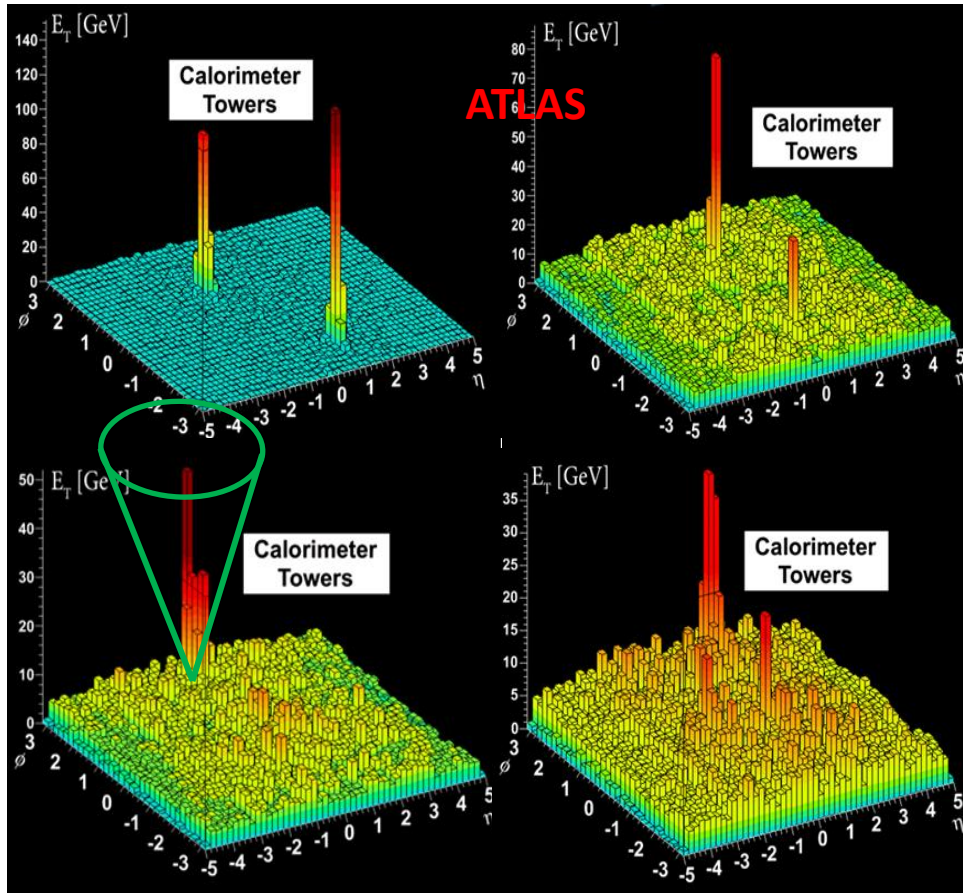
Based on B. Jager, A. Schafer, M. Stratmann, and W. Vogelsang, Phys. Rev. D67, 054005 (2003)
 F. Aversa, P. Chiappetta, M. Greco, and J. P. Guillet, Nucl. Phys. B327, 105 (1989).

Radiative and collisional contributions



- Radiative E loss provides more dominant contributions to R_{AA} , collisional E loss also has sizable contributions to R_{AA} at not-very-high p_T regime and diminishes with increasing p_T .

Dijet asymmetry in PbPb collisions



$$A_J = \frac{E_{J,1} - E_{J,2}}{E_{J,1} + E_{J,2}}, \quad \Delta\phi = |\phi_1 - \phi_2|$$

Generalized k_T family of jet reconstruction algorithms

- (1) Consider all particles in the list, and compute all distances d_{iB} and d_{ij}
- (2) For particle i , find $\min(d_{ij}, d_{iB})$
- (3) If $\min(d_{iB}, d_{ij}) = d_{iB}$, declare particle i to be a jet, and remove it from the list of particles. Then return to (1)
- (4) If $\min(d_{iB}, d_{ij}) = d_{ij}$, recombine i & j into a single new particle. Then return to (1)
- (5) Stop when no particles are left

$$d_{iB} = p_{T,i}^{2p}$$

$$d_{ij} = \min(p_{T,i}^{2p}, p_{T,j}^{2p}) \frac{\Delta R_{ij}^2}{R^2}$$

$$\Delta R_{ij}^2 = (\phi_i - \phi_j)^2 + (\eta_i - \eta_j)^2$$

$p=1$: k_T algorithm

$p=0$: Cambridge/Aachen algorithm

$p=-1$: anti- k_T algorithm